Institute of Space and Aeronautical Science, University of Tokyo
Report No. 547, May 1977

The Flight Dynamics of an Ocean Space Surveying Vehicle

By

Akira AZUMA and Ken-Ichi NASU

Summary: An ocean surveying vehicle will be introduced, which is a remotely piloted vehicle for obtaining oceanographic informations during its operation in a test area of ocean.

The equations of motion of a general submersible and their solutions for perturbed motion will be presented in nonlinearized form. The performance and the flight dynamics of an exemplified vehicle will be discussed and compaired with the operational test results.

SYMBOLS

A_{ij}	Added mass tensor, Table 2 and Table 6.
$A_{0,1,2}$	Coefficients defined by eq. (7.10)
a	Lift slope of fan blade of thruster
$B_{0,1,2}$	Coefficients defined by eq. (7.10)
b	Distance between two thrusters
$C_{0,1,2}$	Coefficients defined by eq. (7.10)
C_D	Drag coefficient
C_F	Force coefficient, eq. (3.1)
C_M	Moment coefficient, eq. (3.1)
C_T	Thrust coefficient, eq. (3.5)
D	Determinant; differential operator of time, $\partial/\partial t$
$D_{0,1,2}$	Coefficents defined by eq. (7.10)
d	Differential operator; distance of vehicle from coordinate fixer, Fig. 10
d_1, d_2	Switching limit of distance, Table 10
e	Exponential symbol, exp.
$\boldsymbol{F}$	Force vector
$\boldsymbol{F}_B$	Buoyant force vector
$\boldsymbol{F}_G$	Gravitational force vector
F_r	Froud number, eq. (4.28)
F_T	Thrust force, eq. (3.8~9)
$\boldsymbol{g}$	Gravity acceleration

* Fujitsu Ltd.

g	Value of gravity acceleration, $\|\boldsymbol{g}\|$
h	Hight of vehicle with respect to coordinate fixer, Fig. 10
I_{ij}	Moment of inertia
i	Running index
$(\boldsymbol{i}, \boldsymbol{j}, \boldsymbol{k})$	Unit vectors with respect to body coordinate system, Fig. 4
$(\boldsymbol{i}_0, \boldsymbol{j}_0, \boldsymbol{k}_0)$	Unit vectors with respect to stationary coordinate system, Fig. 5
$(\boldsymbol{i}_E, \boldsymbol{j}_E, \boldsymbol{k}_E)$	Unit vectors with respect to Earth coordinate system, Fig. 5
$J_{XY,XZ,YZ}$	Products of inertia
j	Running index
$k_{0,1,2,3}$	Coefficients defined by eq. (7.10)
(L, M, N)	Moment components with respect to body coordinate system
M	Mass of vehicle, $M=W/g$
M_{ij}	Generalized mass tensor, Table 5
$\boldsymbol{M}$	Moment vector
$\boldsymbol{M}_B$	Buoyant moment vector
$\boldsymbol{M}_G$	Gravity moment vector
M_T	Thrust moment
$\boldsymbol{n}$	Unit normal vector of elemental surface, positive for outward
$\boldsymbol{n}_V$	Unit vector from coordinate fixer to vehicle eq. (7.2)
O	Origin of body coordinate system
P	Nondimensional parameter defined by eq. (4.29)
p	Pressure of fluid
(p, q, r)	(X, Y, Z) components of $\boldsymbol{\omega}$
Q_i	Generalized force vector, eq. (4.1)
q_i	Generalized coordinate vector, eq. (4.8)
R	Fan radius of thruster; radius of turning
$\boldsymbol{r}$	Position vector of vehicle with respect to Earth coordinate system
$\boldsymbol{r}_B$	Position vector of center of buoyant force
$\boldsymbol{r}_G$	Position vector of center of gravity
$\boldsymbol{r}_{\mathrm{I,II,III}}$	Relative position vector of hydrophones, eq. (7.1)
S	Surface of integration; Disc area of thruster; Laplacian parameter
$S_{0,1,2}$	Characteristic roots, eq. (7.9)
T	Thrust of thruster; Kinetic energy of total system, eq. (4.1)
$\boldsymbol{T}$	Transformation matrix of body angular velocity, eq. (1.4)
$\boldsymbol{T}_B$	Transformation matrix of body coordinate axes, eq. (1.1)
$\boldsymbol{T}_E$	Transformation matrix of Earth coordinate axes, eq. (1.5)
t	Time
$t_{\mathrm{II,III}}$	Time differences among hydrophones, eq. (7.3)
$\boldsymbol{U}$	Velocity of vehicle with respect to body coordinate system, Fig. 4
$\boldsymbol{U}_0$	Velocity of vehicle with respect to stationary coordinate system
$\boldsymbol{U}_E$	Velocity of vehicle with respect to Earth coordinate system
$\boldsymbol{V}$	Relative velocity of vehicle with respect to fluid, eq. (1.10)

V	Volume of integration; absolute value of relative velocity, $\lvert V \rvert$
V_B	External volume of vehicle
V_D	Displacement volume of vehicle
v	Induced velocity of thruster
v_i	(X, Y, Z) components of $\boldsymbol{U}$ and $\boldsymbol{\omega}$
v_i^w	(X, Y, Z) components of $\boldsymbol{V}$ and $\boldsymbol{\omega}$
$\boldsymbol{W}$	Current velocity with respect to body coordinate system
$\boldsymbol{W}_0$	Current velocity with respect to stationary coordinate system
$\boldsymbol{W}_E$	Current velocity with respect to Earth coordinate system
W	Wetted weight of vehicle
W_D	Dry weight of vehicle
(X, Y, Z)	Body coordinate axes, Fig. 3
(X_0, Y_0, Z_0)	Stationary coordinate axes, Fig. 3, Fig. 5.
(X_E, Y_E, Z_E)	Earth coordinate axes, Fig. 5
$(x_{E1,2,3,4}; y_{E1,2,3,4})$	Switching points, Fig. 11
(x_B, y_B, z_B)	(X, Y, Z) components of $\boldsymbol{r}_B$
(x_E, y_E, z_E)	(X_E, Y_E, Z_E) components of $\boldsymbol{r}_E$
(x_G, y_G, z_G)	(X, Y, Z) components of $\boldsymbol{r}_G$
$(x_{\mathrm{I,II,III}}, y_{\mathrm{I,II,III}}, z_{\mathrm{I,II,III}})$	(X, Y, Z) conponents of $\boldsymbol{r}_{\mathrm{I,II,III}}$
α	Angle of attack, Fig. 7
α_{ir}	Transformation tensor of generalized coordinate system, eq. (4.11)
β	Angle of side slip, Fig. 7
β_{ir}	Inverse tensor of α_{ir}, α_{ir}^{-1}
γ_{ijk}	Tensor defined by eq. (4.14)
Δ	Perturbation operator
δ_{ij}	Kronecker's delta
ε_{ijk}	Cyclic delta defined in eq. (4.4)
ζ	Damping ratio, eq. (6.36), (6.39)
η_T	Attenuation factor of thrust reversal
Θ	Elevation angle of vehicle with respect to coordinate fixer, Fig 10
θ	Pitching component in Eulerian angles
λ	Inflow ratio of thruster, eq. (3.5)
Π_i	Generalized force vector with respect to body coordinate system, eq. (4.14)
ρ	Density of fluid
ρ_B	Ensemble density of vehicle
Σ	Summation operator
σ	Solidity of fan of thruster
τ	Elemental volume
Φ	Velocity potential, eq. (4.5)
Φ_i	Velocity potential components, eq. (4.5)
ϕ	Rolling component in Eulerian angles
Ψ	Orientation of current in Earth coordinate system

Ψ_B	Angle of line- of -sight, Table 10
Ψ_{B1}, Ψ_{B2}	Switching limit of angle of line- of -sight Table 10
ψ	Yawing component in Eulerian angles
Ω	Fan speed of thruster
$\boldsymbol{\omega}$	Angular velocity with respect to body coordinate system, Fig. 4
$\boldsymbol{\omega}_E$	Angular velocity of Eulerian angles
ω_n	Undamped natural frequency, eq. (6.36), (6.39)
∇	Gradient operator
$(\ )^{-1}$	Inverse form of ( )
$(\ )^T$	Transposed matrix of ( )
$\Delta(\ )$	Perturbed quantity of ( )
$(\ )_{X,Y,Z}$	(X, Y, Z) components of ( )
$(\ )_{X0,Y0,Z0}$	(X_0, Y_0, Z_0) components of ( )
$(\ )_{X_E,Y_E,Z_E}$	(X_E, Y_E, Z_E) components of ( )
$(\ )_i$	Initial value of ( )
$(\ )_0$	Stationary value of ( )
$(\overline{\ })$	Nondimensional quantity of ( ), eq. (4.18~24)
$(\dot{\ })$	Time derivative of ( ), $\partial(\ )/\partial t$
$(\ )'$	Nondimentional time derivative, $(\ )/\partial\bar{t}$
$(\ )_A$	Differentiation of ( ) with respect to any quantity A, $\partial(\ )/\partial A$
$(X_{(\ )}, Y_{(\ )}, Z_{(\ )})$	Force coefficients defined by eq. (6.12~15) and (6.18~19)
$(L_{(\ )}, M_{(\ )}, N_{(\ )})$	Moment coefficient defined by eq. (6.16~17) and (6.20~23)

§1 Introduction

The ocean space surveying vehicle is one of components of ocean space robot system (briefly called OSR) which is a system for obtaining oceanographic information by using sugmerged vehicles, moored buoys and auxiliary subsystems such as radio and acoustic communication systems, a data processing system, and a mother ship. Planning and development work on this system had been conducted by the Japan Society for the Promotion of Machine Industry (JSPMI) since 1971 and ended March 1976. The design, production and experimental tests of the OSR had been performed by several companies* in Japan with the technical assistance of the OSR project team organized as an advisory group to the Machines and

* Mitsui Ocean Development & Engineering Co., Ltd.
Mitsui Shipbuilding & Engineering Co., Ltd.
Matsushita Communication Industrial Co., Ltd.
Oki Electric Industry Co., Ltd.
Hokushin Electric Works, Ltd.
Mitsubishi Electric Corporation.
Japan Radio Co., Ltd.
Fuyo Ocean Development & Engineering Co., Ltd.

Systems Development Center of JSPMI. The project team consisted of specialists** in respective field of oceanography, instrumentation, electronics, communication, information, structure, and flight dynamics. The one of authors was a member of the project team organized for participating the design, construction and the operation test of the vehicle as consulting staff.

The ocean space surveying vehicle is an unmanned or remotely piloted submersible which has a measuring instrumentation system comprised of various sensors, an automatic homing control system, a data storing and transferring system and a trouble detecting system. Under the navigation of the automatic homing control system the vehicle can descend, land and ascend vertically over a fixed position or positions specified by a coordinate fixer or fixers within a specified interval of time following any one of given flight patterns.

The measuring instrumentation system can measure the ocanographic parameters such as water temperature, electrical conductivity or salinity, concentrations of dissolved oxygen and hydrogen ion (pH), turbidity, pressure and acoustic speed of that area of the sea during its ascending flight, and speed and direction of current during landing on the bottom. Acquired data are stored in a cassette-type tape-recorder, and then transmitted to a data processing center through a radio communication system by relaying with the similar communication system on the buoy moored around the measured area while the vehicle is floating on the surface of the sea.

The coordinate fixer, which is sank on the bottom of the sea prior to the operation, has an acoustic transmitter and can, therefore, be a source of ultrasonic signal for every one second. The vehicle can detect the signals by three hydrophones installed on the respective vehicle and by the help of the automatic homing control system approach an upright axis of radiation cone of the ultrasonic waves by searching the direction of the acoustic source with respect to the body axis of the vehicle.

The vehicle can also detect its troubles being objectionable for regular operation such as abnormal attitude, appreciable electric boltage drop, inundation and so on. If any trouble is actually detected, then the operation is discontinued and the vehicle is surfaced in obedience to an emergency operation corresponding to the degree of trougle.

The functional relationships among the all systems can be seen in Fig. 1. The

** Dr. Shigeru Watanabe, Professor, Univ. of Tokyo.
Dr. Toshihiko Teramoto, Professor, Univ of Tokyo.
Dr. Akira Azuma, Professor, Univ. of Tokyo.
Dr. Hirofumi Miura, Assor. Professor, Univ. of Tokyo.
Mr. Fumio Miyata, Research Associate, Univ. of Tokyo.
Dr. Chikara Sato, Professor, Keio University.
Dr. Shuhei Aida, Assoc. Professor, Univ. of Electrocommunications.
Dr. Tomio Emura, Manager, Japan Marine Science and Technology Center.
Dr. Takuya Homma, Chief manager, Electrotechnical Lab. of Ministry of International Trade and Industry.
Mr. Koji Yada, Manager, Electrotechnical Lab. of Ministry of International Trade and Industry.

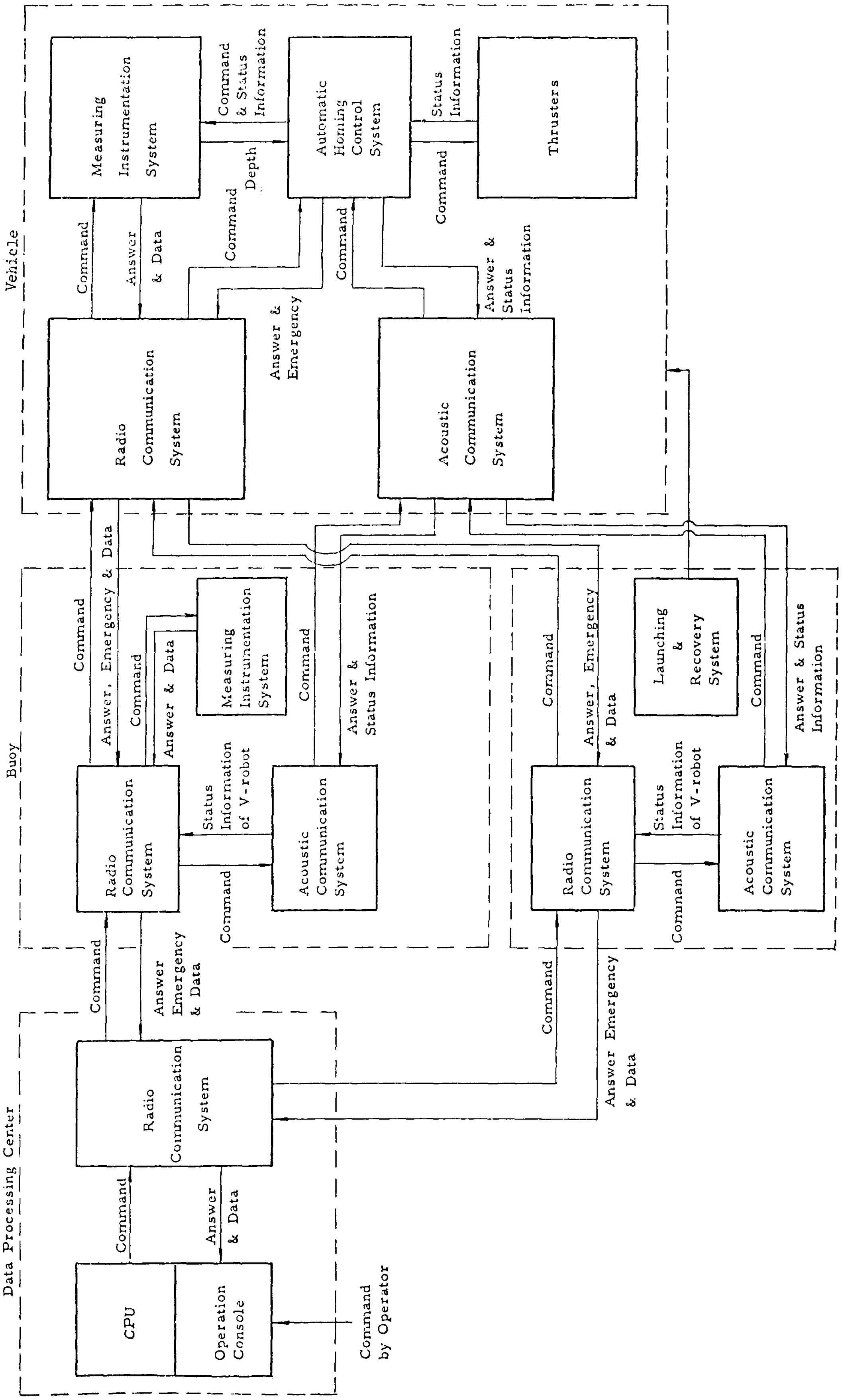

FIG. 1. Functional block diagram

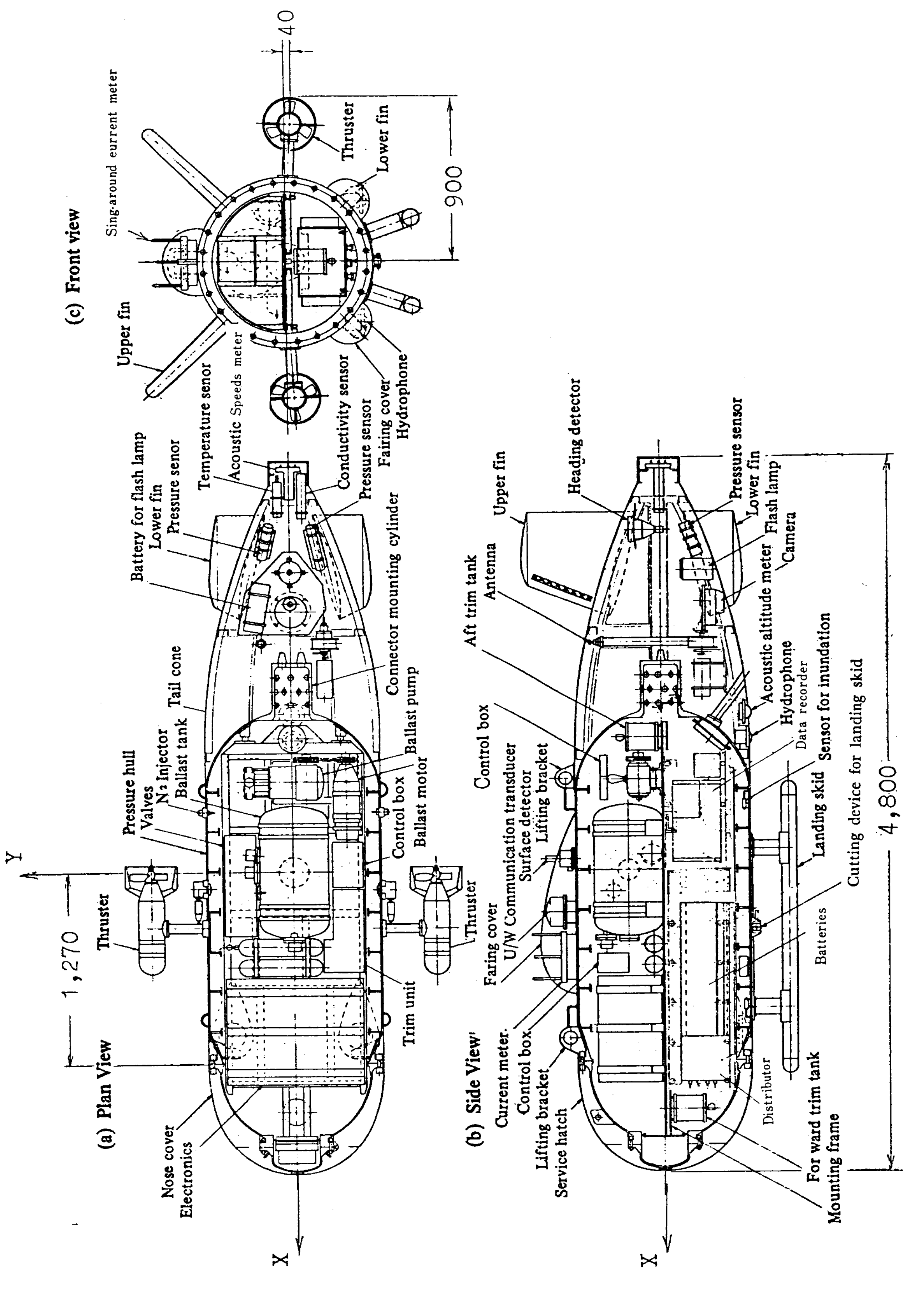

FIG. 2. General configuration of the vehicle

TABLE 1. Specifications of main body and suxiliary devices of the V-robot

	Item		Description
Main Specification	Total length		4.800 m
	Total width		2.160 m
	Total height with antenna extended		4.12 m
	with antenna retracted		1.760 m
	Total body volume (or external volume), V_B		3.493 m^3
	Displacement volume, V_D		2.68 m^3
	Dry weight, in air		2.75 ton$\pm$40 kg
	Wetted weight, W		3.580 ton$\pm$40 kg
	Center of buoyant force		
	Horizonal (from top of the body)		1.86 m (normal) 1.86 m (emergency)
	Vertical (downward from center of the body)		0 m (normal) $-$0.01 m (emergency)
	Center of gravity		
	Horizontal (from top of the body)		1.86 m (normal) 1.86 m (emergency)
	Vertical (downward from center the of body)		0.05 m (normal) 0.03 m (emergency)
	Pressure hull	Length	3.38 m
		Diameter	1.11 m
		Displacement	2.35 m^3
	Outer Structure	Length of nose cover	1.05 m
		Length of tail cone	1.71 m
		Area of upper fins*	0.74 m$^2\times$2
		Area of lower fins*	0.44 m$^2\times$2
		Fin profile	NACA 0015
	Propulsion	Type	Shrouded propellor
		Number of thrusters	2
		Number of blades	3
		Operation	On-off
		Normal thrust	22 kg at speed of 2 m/sec. 51 kg at rest
		Reverse thrust	30 kg at rest
		Motor	DC 5 HP (Max.) 2 HP (at set point)
		Shroud diameter	0.360 m
Auxiliary Devices and Other Accessories	Buoyancy Adjustment Device	Type	Flooding and draining with water piston pump
		Volume of ballast tank	96 l
		Pump	Piston pump
		Draining rate	54 cc/rev at 720 rpm
		Drive motor	DC 5 HP at 3,500 rpm
		Valve unit	Electro magnetic type with relief and check valves
	Emergency Surfacing Device	Air bottle Pressure	300 kg/cm^2
		Volume	4 $l\times$2
		Wasted ballast	64 kg
	Landing Skid and Others	Droppable skid Length	1.90 m
		Weight	97 kg
		Hooks	2
		Retractable antenna	1
	Power Sources	Battery for pump and thrusters	Silver oxide 100 V$\times$140 AH
		Battery for instruments	+24 V$\times$100 AH$-$24 V$\times$16 AH
		Emergency battery	Primary +24 V

TABLE 1 (Continued)

	Item		Description
Automatic Homing Control System	Position Detecting Unit	Hydrophone	3
		Acoustic altitude meter	1
		Declinometer	1
		Attitude sensor	2
		Control unit	1
	Others	Surface detector	1
		Sensor for inundation	2
		Timer for setting of time-out	1

* Considered to be extended to the furelage center line

general configuration and the detailed specification of the vehicle are shown in Fig. 2 and Table1 respectively.

Further detailed description on the design philosophy, general configuration, and the experimental test results can be found in Ref. 1 and 2.

Three sets of Cartesian coordinate systems are used in this paper for describing the dynamics. One set is fixed to the vehicle and is known as "body coordinate system" or (X, Y, Z) axes, and other two sets are respectively "stationary coordinate system" or (X_0, Y_0, Z_0) axes and "earth coordinate system" or (X_E, Y_E, Z_E) axes the both of which are fixed in the stationately space.

The orientation of the body axes can be determined from the stationary axes (X_0, Y_0, Z_0) through Eulerian angles, after three consecutive rotations, ψ, θ and ϕ as shown in Fig. 3. The sign of the angle is specified by giving the axis about which the rotation is taken as follows:

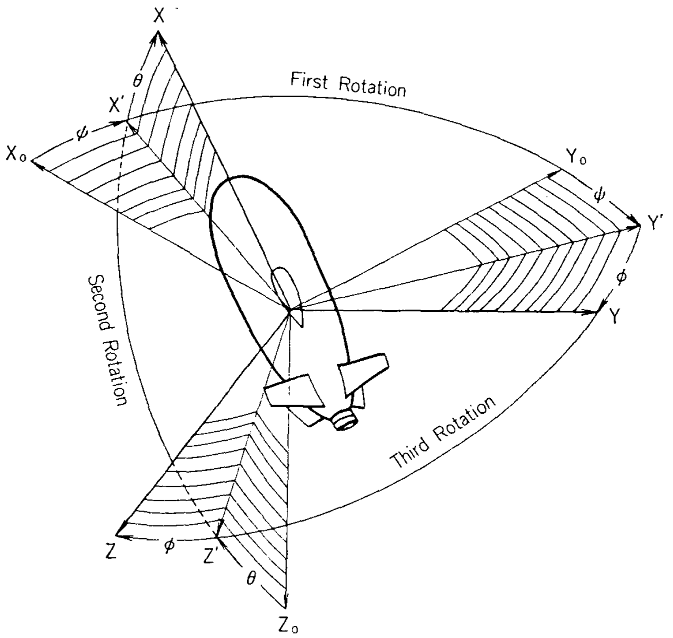

FIG. 3. Eulerian angles between sationary axes, (X_0, Y_0, Z_0) and body axes, (X, Y, Z).

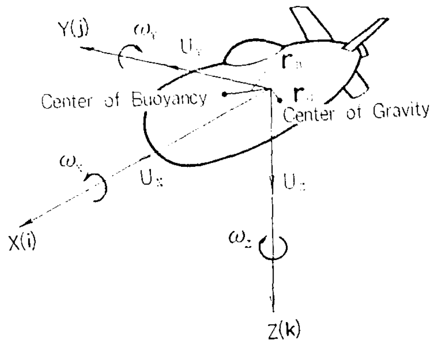

FIG. 4. Linear and angular velocities along the body axes.

ψ: angle between X_0 and intersection X_0Y_0 and XZ_0 planes (rotation about Z_0)
θ: angle between intersection of X_0Y_0 and XZ_0 planes and X (rotation about Y')
ϕ: angle between intersection of YZ and X_0Y_0 planes and Y (rotation about X).

The transformation matrix, T_B, between (X_0, Y_0, Z_0) and (X, Y, Z) systems can be obtained from the direction cosine between them as follows:

T_B^{-1} \ T_B	X	Y	Z
X_0	$\cos\theta\cos\psi$	$\cos\psi\sin\phi\sin\theta-\sin\psi\cos\phi$	$\cos\psi\cos\phi\sin\theta+\sin\psi\sin\phi$
Y_0	$\cos\theta\sin\psi$	$\sin\psi\sin\phi\sin\theta+\cos\psi\cos\phi$	$\sin\psi\cos\phi\sin\theta-\cos\psi\sin\phi$
Z_0	$-\sin\theta$	$\sin\phi\cos\theta$	$\cos\theta\cos\phi$

(1.1)

By referring to Fig. 4 the components of linear and angular velocities are respectively given by

$$\boldsymbol{U}_0=\boldsymbol{T}_B^{-1}\cdot\boldsymbol{U}$$

or

$$\left.\begin{aligned}\begin{pmatrix}U_{X_0}\\U_{Y_0}\\U_{Z_0}\end{pmatrix}&=\begin{pmatrix}\cos\theta\cos\psi\\\cos\theta\sin\psi\\-\sin\theta\end{pmatrix}U_X+\begin{pmatrix}\cos\psi\sin\phi\sin\psi-\sin\psi\cos\phi\\\sin\psi\sin\phi\sin\theta-\cos\psi\cos\phi\\\sin\phi\cos\theta\end{pmatrix}U_Y\\&\quad+\begin{pmatrix}\cos\psi\cos\phi\sin\theta+\sin\psi\sin\phi\\\sin\psi\cos\phi\sin\theta-\cos\psi\sin\phi\\\cos\theta\cos\phi\end{pmatrix}U_Z\end{aligned}\right\}\tag{1.2}$$

and

$$\omega=\boldsymbol{T}\cdot\boldsymbol{\omega}_E$$

or

$$\begin{pmatrix}\omega_X\\\omega_Y\\\omega_Z\end{pmatrix}=\begin{pmatrix}\dot\theta-\dot\psi\sin\theta\\\dot\theta\cos\phi+\dot\psi\cos\theta\sin\phi\\\dot\psi\cos\theta\cos\phi-\dot\theta\sin\phi\end{pmatrix}.\tag{1.3}$$

where $\boldsymbol{T}$ is the transformation matrix between the body angular velocity, $\boldsymbol{\omega}$, and the rate of Eulerian angles, $\boldsymbol{\omega}_E=(\dot{\phi}, \dot{\theta}, \dot{\psi})^T$,

$$\boldsymbol{T}=\begin{pmatrix} 1, & 0, & -\sin\theta \\ 0, & \cos\phi, & \cos\theta\sin\phi \\ 0, & -\sin\phi, & \cos\theta\cos\phi \end{pmatrix}. \tag{1.4}$$

The earth axes, (X_E, Y_E, Z_E), are oriented such as that X_E axis is pointed to north and Z_E axis is directed to the center of the earth as shown in Fig. 5. If the orientation of the X_0 axis is represented by an angle denoted by Ψ with respect to X_E axis, then the angular transformation between two sets of the coordinate system will be attained by the following transformation:

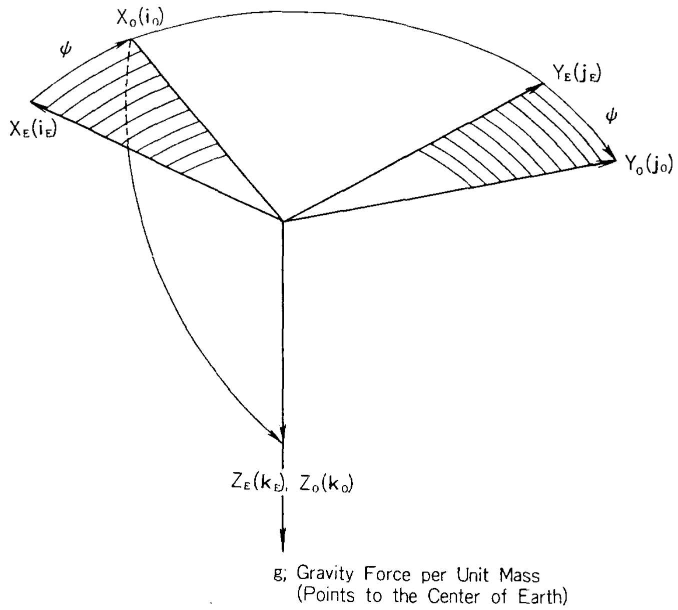

FIG. 5. Orientation of earth axes

T_E^{-1} \ T_E	X_0	Y_0	Z_0
X_E	$\cos\Psi$	$-\sin\Psi$	0
Y_E	$\sin\Psi$	$\cos\Psi$	0
Z_E	0	0	1

(1.5)

Since the earth's rotation is negligibly slow comparing with the angular velocity of the vehicle motion, the earth axes are considered to be Galilean or inertial coordinate system fixed in stationary space.

The velocity components along the (X_E, Y_E, Z_E) axes can be given by

$$\boldsymbol{U}_E=\boldsymbol{T}_E^{-1}\cdot\boldsymbol{U}_0$$

or

$$\begin{pmatrix} U_{X_E} \\ U_{Y_E} \\ U_{Z_E} \end{pmatrix}=\begin{pmatrix} \cos\Psi \\ \sin\Psi \\ 0 \end{pmatrix}U_{X_0}+\begin{pmatrix} -\sin\Psi \\ \cos\Psi \\ 0 \end{pmatrix}U_{Y_0}+\begin{pmatrix} 0 \\ 0 \\ 1 \end{pmatrix}U_{Z_0}. \tag{1.6}$$

Then the position of the body with respect to the earth axes can be calculated by integrating the above equation with time as

$$r_E(t)=\int_{t_i}^{t} U_E dt + r_{E,i}$$

or

$$\begin{pmatrix} x_E \\ y_E \\ z_E \end{pmatrix} = \int_{t_i}^{t} \begin{pmatrix} U_{X_E} \\ U_{Y_E} \\ U_{Z_E} \end{pmatrix} dt + \begin{pmatrix} x_{E,i} \\ y_{E,i} \\ z_{E,i} \end{pmatrix} \tag{1.7}$$

where the subscript i shows initial state of the related quantities.

The current of the sea, W_E, can usually be shown by the components of the earth axes as (W_X, W_Y, W_Z). Then the current components along (X_0, Y_0, Z_0) and (X, Y, Z) axes are given as

$$W_0 = T_E \cdot W_E$$

or

$$\begin{pmatrix} W_{X_0} \\ W_{Y_0} \\ W_{Z_0} \end{pmatrix} = \begin{pmatrix} \cos \Psi \\ -\sin \Psi \\ 0 \end{pmatrix} W_{X_E} + \begin{pmatrix} \sin \Psi \\ \cos \Psi \\ 0 \end{pmatrix} W_{Y_E} + \begin{pmatrix} 0 \\ 0 \\ 1 \end{pmatrix} W_{E_E} \tag{1.8}$$

and

$$W = T_B \cdot T_E \cdot W_E$$

or

$$\begin{pmatrix} W_X \\ W_Y \\ W_Z \end{pmatrix} = \left\{ \begin{bmatrix} \cos\theta\cos\psi\cos\Psi - \cos\theta\sin\psi\sin\Psi \\ (\cos\psi\sin\phi\sin\theta - \sin\psi\cos\phi)\cos\Psi \\ \quad -(\sin\psi\sin\phi\sin\theta + \cos\psi\cos\phi)\sin\Psi \\ (\cos\psi\cos\phi\sin\theta + \sin\psi\sin\phi)\cos\Psi \\ \quad -(\sin\psi\cos\phi\sin\theta - \cos\psi\sin\phi)\sin\Psi \end{bmatrix} W_{X_E} \right.$$
$$+ \begin{bmatrix} \cos\theta\cos\psi\sin\Psi + \cos\theta\sin\psi\cos\Psi \\ (\cos\psi\sin\phi\sin\theta - \sin\psi\cos\phi)\sin\Psi \\ \quad +(\sin\psi\sin\phi + \cos\psi\cos\phi)\cos\Psi \\ (\cos\psi\cos\phi\sin\theta + \sin\psi\sin\phi)\sin\Psi \\ \quad +(\sin\psi\cos\phi\sin\theta - \cos\psi\sin\phi)\cos\Psi \end{bmatrix} W_{Y_E} \tag{1.9}$$
$$\left. + \begin{pmatrix} -\sin\theta \\ \sin\phi\cos\theta \\ \cos\theta\cos\phi \end{pmatrix} W_{Z_E}. \right\}$$

Then the relative velocity of the vehicle with respect to the fluid can be given by

$$V=U-W$$

or

$$\begin{pmatrix} V_X \\ V_Y \\ V_Z \end{pmatrix}=\begin{pmatrix} U_X-W_X \\ U_Y-W_Y \\ U_Z-W_Z \end{pmatrix}. \tag{1.10}$$

Unit vectors of these axes are defined as follows:

$(\boldsymbol{i}, \boldsymbol{j}, \boldsymbol{k})$; (X, Y, Z) axes
$(\boldsymbol{i}_0, \boldsymbol{j}_0, \boldsymbol{k}_0)$; (X_0, Y_0, Z_0) axes
$(\boldsymbol{i}_E, \boldsymbol{j}_E, \boldsymbol{k}_E)$; (X_E, Y_E, Z_E) axes.

§2 Hydrostatic and Body Forces and Moments

Hydrostatic force and moment acting on a stationary body immersed in the fluid are resulted from the static pressure, p, over the external surface of the body as follows:

$$\left.\begin{aligned} \boldsymbol{F}_B&=-\int_S p\boldsymbol{n}dS=-\int_V \nabla p d\tau \\ \boldsymbol{M}_B&=-\int_S p\boldsymbol{r}\times\boldsymbol{n}dS=-\int_V \boldsymbol{r}\times(\nabla p)d\tau=\boldsymbol{r}_B\times\boldsymbol{F}_B \end{aligned}\right\} \tag{2.1}$$

where $\boldsymbol{r}$ and $\boldsymbol{n}$ are the position vector and the normal vector of the elemental surface dS respectively, $d\tau$ is the elemental volume, and $\boldsymbol{r}_B$ is the center of buoyant force. When the fluid is a single medium and is barotropic, the gradient of pressure is, from Bernoullis theorem, equal to the gravity force (shown in Fig. 5) per unit volume, $\rho\boldsymbol{g}$, or

$$\nabla p=\rho\boldsymbol{g} \tag{2.2}$$

where $\rho(=104.5\ \text{kg}\ \text{sec}^2/\text{m}^4)$ is the fluid density, and may be assumed constant in a specified area. Thus the force and moment can again be written as

$$\boldsymbol{F}_B=-\rho\boldsymbol{g}V_B=-\boldsymbol{k}_E\rho g V_B$$

or

$$\begin{pmatrix} F_{B,X} \\ F_{B,Y} \\ F_{B,Z} \end{pmatrix}=\begin{pmatrix} \sin\theta \\ -\cos\theta\sin\phi \\ -\cos\theta\cos\phi \end{pmatrix}\rho g V_B \tag{2.3}$$

and

$$\boldsymbol{M}_B=\boldsymbol{r}_B\times\boldsymbol{F}_B$$

or

$$\begin{pmatrix} M_{B,X} \\ M_{B,Y} \\ M_{B,Z} \end{pmatrix} = \begin{pmatrix} -y_B \cos\theta \cos\phi + z_B \cos\theta \sin\phi \\ z_B \sin\theta + x_B \cos\theta \cos\phi \\ -x_B \cos\theta \sin\phi - y_B \sin\theta \end{pmatrix} \rho g V_B \tag{2.4}$$

where $V_B(=3.49\ \mathrm{m}^3)$ is the volume of total body or external volume of the vehicle. The external volume is comprised of displacement volume, $V_D(=2.68\ \mathrm{m}^3)$, which is the volume occupied by both the sealed space against water and the vehicle materials themselves, and of vacant volume, $V_B - V_D(=0.81\ \mathrm{m}^3)$, which is occupied by the water inundated into the vehicle outside of the sealed space. Thus the buoyant force is considered here to be the hydrostatic force acting on the external surface of the vehicle. The location of center of buoyant force, $\boldsymbol{r}_B$, is also considered to be that of the total body volume.

The gravity force is, as shown in Fig. 5, directed to Z_E axis and acts to the center of gravity $\boldsymbol{r}_G$. Thus the force and moment due to the gravitational acceleration can respectively be given by

$$\boldsymbol{F}_G = W\boldsymbol{k}_E = \rho_B g V_B \boldsymbol{k}_E$$

or

$$\begin{pmatrix} F_{G,X} \\ F_{G,Y} \\ F_{G,Z} \end{pmatrix} = \begin{pmatrix} -\sin\theta \\ \cos\theta \sin\phi \\ \cos\theta \cos\phi \end{pmatrix} \rho_B g V_B \tag{2.5}$$

and

$$\boldsymbol{M}_G = \boldsymbol{r}_G \times \boldsymbol{F}_G$$

or

$$\begin{pmatrix} M_{G,X} \\ M_{G,Y} \\ M_{G,Z} \end{pmatrix} = \begin{pmatrix} y_G \cos\theta \cos\phi - z_G \cos\theta \sin\phi \\ -z_G \sin\theta - x_G \cos\theta \cos\phi \\ x_G \cos\theta \sin\phi + y_G \sin\theta \end{pmatrix} \rho_B g V_B \tag{2.6}$$

where $\boldsymbol{r}_G$ is the center of gravity of the wetted weight W which is the dry weight of the vehicle itself in the air, W_D, plus the weight of the water inundated into the vehicle or

$$W = W_D + \rho(V_B - V_D)g, \tag{2.7}$$

and where $\rho_B(=104.5 \pm 1.2\ \mathrm{kgsec^2/m^4})$ is the ensemble density of the vehicle based on the total volume or

$$\rho_B = W/gV_B. \tag{2.8}$$

The mass of the inundated water may be considered to be a part of the body moving with the vehicle so that the mass, mass moment, and moment of inertia of the vehicle should be comprised of both the body materials and this inundated water.

For small perturbation the derivatives of these forces and moments with respect to the related variables are, then, given by

$$\begin{pmatrix} F_{B,X}-F_{G,X} \\ F_{B,Y}-F_{G,Y} \\ F_{B,Z}-F_{G,Z} \end{pmatrix}_{\theta} = (\rho-\rho_B) g V_B \begin{pmatrix} \cos\theta \\ \sin\theta\sin\phi \\ \sin\theta\cos\phi \end{pmatrix} \tag{2.9}$$

$$\begin{pmatrix} F_{B,X}-F_{G,X} \\ F_{B,Y}-F_{G,Y} \\ F_{B,Z}-F_{G,Z} \end{pmatrix}_{\phi} = (\rho-\rho_B) g V_B \begin{pmatrix} 0 \\ -\cos\theta\cos\phi \\ \cos\theta\sin\phi \end{pmatrix} \tag{2.10}$$

$$\begin{pmatrix} M_{B,X}-M_{G,X} \\ M_{B,Y}-M_{G,Y} \\ M_{B,Z}-M_{G,Z} \end{pmatrix}_{\theta} = g V_B \begin{pmatrix} (\rho y_B-\rho_B y_G)\sin\theta\cos\phi-(\rho z_B-\rho_B z_G)\cos\theta\sin\phi \\ (\rho z_B-\rho_B z_G)\cos\theta-(\rho x_B-\rho_B x_G)\sin\theta\cos\phi \\ (\rho x_B-\rho_B x_G)\sin\theta\sin\phi-(\rho y_B-\rho_B y_G)\cos\theta \end{pmatrix} \tag{2.11}$$

$$\begin{pmatrix} M_{B,X}-M_{G,X} \\ M_{B,Y}-M_{G,Y} \\ M_{B,Z}-M_{G,Z} \end{pmatrix}_{\phi} = g V_B \begin{pmatrix} (\rho y_B-\rho_B y_G)\cos\theta\sin\phi+(\rho z_B-\rho_B z_G)\cos\theta\cos\phi \\ -(\rho x_B-\rho_B x_G)\cos\theta\sin\phi \\ -(\rho x_B-\rho_B x_G)\cos\theta\cos\phi \end{pmatrix} \tag{2.12}$$

where subscripts θ and ϕ show the partial differentiation of ( ) with respect to the related quantities,

$$(\ )_{\phi}=\partial(\ )/\partial\phi$$
$$(\ )_{\theta}=\partial(\ )/\partial\theta.$$

§3 Hydrodynamic Forces and Moment

It is very much difficult to estimate the hydrodynamic characteristics of the vehicle having a complex shape of slender like body the fineness ratio of which is 3.77.

The added mass effects on the immersed body in unsteady motion have been calculated from the potential theory as a summation of simply idealized forms, each of which can be treated mathematically [*3*]. The result is given in Table 2 in both dimensional form and nondimensional form by dividing with ρV_B for mass, $\rho V_B^{4/3}$ for mass moment, and $\rho V_B^{5/3}$ for moment of inertia, where V_B is, as stated before, the external volume occupied by total volume of the vehicle. Subscripts of combinations of number 1 to 6 show respective comonent defined in Ref. 3 and in Table 6 in the subsequent section of this paper.

The steady hydrodynamic forces and moments have been evaluated both by the wind tunnel test, conducted at Institute of Space and Aeronautical Science, University of Tokyo and by the water tunnel test conducted at Mitsui Shipbuilding & Engineering Co., Ltd. The results are shown in Fig. 6 as coefficient forms nondimensionalized by dividing with dynamic pressure, $(1/2)\rho V^2=(1/2)\rho(U-W)^2$, times reference area, $V_B^{2/3}$, for forces and times reference volume, V_B, for moments as follows:

$$\left.\begin{aligned} C_{F_{X,Y,Z}}&=F_{X,Y,Z}/(1/2)\rho V^2 V_B^{2/3} \\ C_{M_{X,Y,Z}}&=M_{X,Y,Z}/(1/2)\rho V^2 V_B \end{aligned}\right\} \tag{3.1}$$

where

$$V=|\boldsymbol{V}|=|\boldsymbol{U}-\boldsymbol{W}|$$

TABLE 2 Added masses

Dimensional values		Nondimensional values	
A_{11}	32.0 kgsec²/m	$\bar{A}_{11}=A_{11}/\rho V_B$	0.088
A_{22}	383.0 kgsec²/m	$\bar{A}_{22}=A_{22}/\rho V_B$	1.049
A_{33}	377.0 kgsec²/m	$\bar{A}_{33}=A_{33}/\rho V_B$	1.033
A_{13}	0 kgsec²/m	$\bar{A}_{13}=A_{13}/\rho V_B$	0
A_{15}	0 kgsec²	$\bar{A}_{15}=A_{15}/\rho V_B^{4/3}$	0
A_{24}	0 kgsec²	$\bar{A}_{24}=A_{24}/\rho V_B^{4/3}$	0
A_{26}	−98.5 kgsec²	$\bar{A}_{26}=A_{26}/\rho V_B^{4/3}$	−0.173
A_{35}	94.3 kgsec²	$\bar{A}_{35}=A_{35}/\rho V_B^{4/3}$	0.170
A_{44}	45.3 kgsec²m	$\bar{A}_{44}=A_{44}/\rho V_B^{5/3}$	0.054
A_{55}	504.3 kgsec²m	$\bar{A}_{55}=A_{55}/\rho V_B^{5/3}$	0.600
A_{66}	507.0 kgsec²m	$\bar{A}_{66}=A_{66}/\rho V_B^{5/3}$	0.603
A_{46}	0 kgsec²m	$\bar{A}_{46}=A_{46}/\rho V_B^{5/3}$	0

$\rho=104.5$ kgsec²/m⁴, $V_B=3.493$ m³, $\rho V_B=365$ kgsec²/m,
$\rho V_B^{4/3}=554$ kgsec², $\rho V_B^{5/3}=840$ kgmsec³

TABLE 3 Coefficient and their derivatives of hydrodynamic forces and moments

Items	Values	Items	Values
$C_{F_{X,0}}$	−0.13	$C_{M_{Y,0}}$	−0.02
$C_{F_{X,\alpha}}$	0.10	$C_{M_{Y,\alpha}}$	0.40
$C_{F_{X,\beta}}$	0.10	$C_{M_{Y,\dot{\alpha}}}$	−0.745
		$C_{M_{Y,q}}$	−2.43
$C_{F_{Y,0}}$	0		
$C_{F_{Y,\beta}}$	−1.8	$C_{M_{Z,0}}$	0
$C_{F_{Y,r}}$	2.10	$C_{M_{Z,\beta}}$	−0.40
		$C_{M_{Z,\dot{\beta}}}$	0.745
$C_{F_{Z,0}}$	0	$C_{M_{Z,Y}}$	−2.43
$C_{F_{Z,\alpha}}$	−1.8	$C_{M_{Z,r}}$	−1.57
$C_{F_{Z,q}}$	−2.1		
		$\bar{F}_{T_{X,0}}$	0.0285/P
$C_{M_{X,0}}$	0	$\bar{F}_{T_{X,U_X}}$	−0.0183/P
$C_{M_{X,\beta}}$	0.029	$M_{T_{Z,r}}$	0.00645/P
$C_{M_{X,p}}$	−1.05		
$C_{M_{X,r}}$	0		

TABLE 4 Thrust force and its moment*

Items	Force	Moment
Forward drive	$F_{T_X}=(T_R+T_L)_F$ $=\rho S(R\Omega)^2(C_{T_R}+C_{T_L})_F$	$M_{T_Z}=(b/2)(T_L-T_R)_F$ $=\rho S(R\Omega)^2(C_{T_L}-C_{T_R})_F$
Backward drive	$-F_{T_X}=(T_R+T_L)_B$ $=\rho S(R\Omega)^2(C_{T_R}+C_{T_L})_B$	$-M_{T_Z}=(b/2)(T_L-T_R)_B$ $=\rho S(R\Omega)^2(C_{T_L}-C_{T_R})_B$
Right-turn drive	$F_{T_Z}=T_{L,F}-T_{R,B}$ $=\rho S(R\Omega)^2(C_{T_{L,F}}-C_{T_{R,B}})$	$M_{T_Z}=(b/2)(T_{L,F}+T_{R,B})$ $=(b/2)\rho S(R\Omega)^2(C_{T_{L,F}}+C_{T_{R,B}})$
Left-turn drive	$F_{T_Z}=T_{R,F}-T_{L,B}$ $=\rho S(R\Omega)^2(C_{T_{R,F}}-C_{T_{L,B}})$	$-M_{T_Z}=(b/2)(T_{R,F}+T_{L,B})$ $=(b/2)\rho S(R\Omega)^2(C_{T_{R,F}}+C_{T_{L,B}})$

* Subscript R and L show the right- and left-hand thrusters respectively and subscript F and B show forward- and backward- drives respectively.

The angle of attack, α, and the side slip angle, β, are defined in Fig. 7.

Coefficients of hydrodynamic damping forces and moments have been evaluated by the dynamic or forcedly oscillating model test in the said water tunnel.

The above all coefficients at zero angle of attack and zero angle of side slip and their derivatives with respect to state variables of the vehicle motion are given in Table 3 in which

$$\left.\begin{array}{ll}(\ )_\alpha=\partial(\ )/\partial\alpha, & (\ )_\beta=\partial(\ )/\partial\beta \\ (\ )_{\dot\alpha}=\partial(\ )/\partial(\dot\alpha V_B^{1/3}/V), & (\ )_{\dot\beta}=\partial(\ )/\partial(\dot\beta V_B^{1/3}/V) \\ (\ )_{p,q,r}=\partial(\ )/\partial\{(p,q,r)(V_B^{1/3}/V)\} & \end{array}\right\} \quad (3.2)$$

and

$$\bar{U}_0=U_0/\sqrt{V_B^{1/3}g}. \quad (3.3)$$

Two ducted thrusters installed on opposite sides of fuselage give the thrust and the yawing moment to the vehicle. When one thruster is driven in reversed direction the thrust of that thruster generates negative thrust so that the drive forces, F_{T_X}, and moments, M_{T_Z}, can be given as listed in Table 4. It must be remembered that, as shown in Fig. 1, the vertical position of the thruster nearly coincides with the center of gravity position so that any pitching moment is not introduced by the operation of the thrusters.

The thrust T of each thruster can be expressed by using the thrust coefficient as[5,6]

$$T=\rho S(R\Omega)^2C_T \quad (3.4)$$

where

$$\left.\begin{array}{l}C_T=C_{T_0}+C_{T_\lambda}\lambda \\ C_{T_\lambda}\cong -a\sigma/4 \\ \lambda=(v+V)/R\Omega \\ v/R\Omega=(1/2)\{-(V/R\Omega)+\sqrt{(V/R\Omega)^2+4C_T}\},\end{array}\right\} \quad (3.5)$$

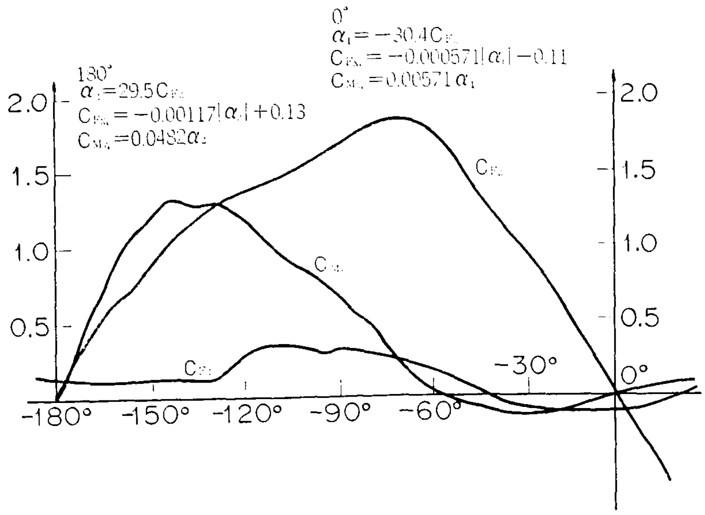

(a) For angle of attack

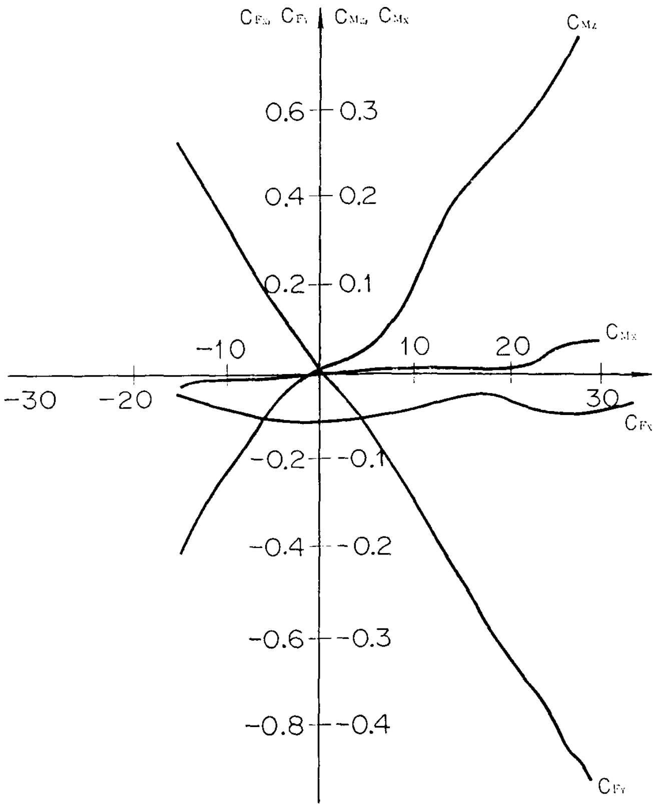

(b) For angle of side slip

FIG. 6. Hydrodynamic characteristics for the robot

and where a is the lift slope of the blade, is the solidity of the rotor of thruster, V is the relative axial speed of the thruster with respect to the surrounding fluid, $R\Omega$ is the tip speed of the blades, v is the induced velocity of the thruster and λ is called "inflow ratio". For respective thruster the inflow ratio can be given as follows:

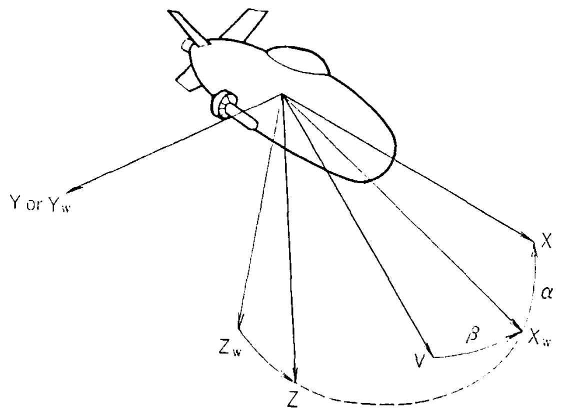

FIG. 7. Angle of attack and side slip angle

$$\left.\begin{aligned} \lambda_{R,F}&=(v_{R,F}+V_X-br/2)/R\Omega \\ \lambda_{L,F}&=(v_{L,F}+V_X+br/2)/R\Omega \\ \lambda_{R,B}&=(v_{R,B}-V_X+br/2)/R\Omega \\ \lambda_{L,B}&=(v_{L,B}-V_X-br/2)/R\Omega \end{aligned}\right\} \quad (3.6)$$

where b is the distance between two thrusters, subscripts R and L show right- and left-hand thrusters respectively and subscripts F and B show forward and backward drives respectively. By assuming that the C_{T_0} is reduced by $\eta_T C_{T_0}$ in reversed direction and that the derivative of the thrust with respect to the inflow ratio is constant throughout any operational condition, the thrust coefficient may be expressed as

$$\left.\begin{aligned} C_{T_{R,F}}&=C_{T_0}+C_{T_\lambda}\lambda_{R,F} \\ C_{T_{L,F}}&=C_{T_0}+C_{T_\lambda}\lambda_{L,F} \\ C_{T_{R,B}}&=C_{T_0}\eta_T+C_{T_\lambda}\lambda_{R,B} \\ C_{T_{L,B}}&=C_{T_0}\eta_T+C_{T_\lambda}\lambda_{L,B}. \end{aligned}\right\} \quad (3.7)$$

Substituting equations (3.6) and (3.7) into the expressions of thrust forces and moments given in Table 4 and, then, nondimensionalizing with $\rho S(R\Omega)^2$ for force and $\rho S(R\Omega)^2 V_B^{1/3}$ for moment, they yield

$$\left.\begin{aligned} &\left.\begin{aligned} \bar{F}_{T_X}&=F_{T_X}/\rho S(R\Omega)^2=2C_{T_0}+C_{T_\lambda}(v_{R,F}+v_{L,F}+2V_X)/R\Omega \\ \bar{M}_{T_Z}&=M_{T_Z}/\rho S(R\Omega)^2 V_B^{1/3}=(b/2V_B^{1/3})C_{T_\lambda}(br/R\Omega) \end{aligned}\right\} \text{forward drive} \\ &\left.\begin{aligned} -\bar{F}_{T_X}&=-F_{T_X}/\rho S(R\Omega)^2=2C_{T_0}\eta_T+C_{T_\lambda}(v_{R,B}+v_{L,B}-2V_X)/R\Omega \\ -\bar{M}_{T_Z}&=-M_{T_Z}/\rho S(R\Omega)^2 V_B^{1/3}=-(b/2V_B^{1/3})C_{T_\lambda}(br/R\Omega) \end{aligned}\right\} \text{backward drive} \\ &\left.\begin{aligned} \bar{F}_{T_X}&=C_{T_0}(1-\eta_T)+C_{T_\lambda}(v_{L,F}-v_{R,B}+2V_X)/R\Omega \\ \bar{M}_{T_Z}&=(b/2V_B^{1/3})\{C_{T_0}(1+\eta_T)+C_{T_\lambda}(v_{L,F}+v_{R,B}+br)/R\Omega\} \end{aligned}\right\} \text{right-turn drive} \\ &\left.\begin{aligned} \bar{F}_{T_X}&=C_{T_0}(1-\eta_T)+C_{T_\lambda}(v_{R,F}-v_{L,B}+2V_X)/R\Omega \\ -\bar{M}_{T_Z}&=(b/2V_B^{1/3})\{C_{T_0}(1+\eta_T)+C_{T_\lambda}(v_{R,F}+v_{L,B}-br)/R\Omega\}. \end{aligned}\right\} \text{left-turn drive} \end{aligned}\right\} \quad (3.8)$$

Then the nondimensional derivatives with respect to the related variables are given by

$$\left.\begin{aligned} \bar{F}_{TX,U_X} &= \partial\bar{F}_{TX}/\partial\bar{U}_X \cong 2C_{T\lambda}/(\overline{R\Omega}) \\ \bar{F}_{TX,W_X} &= \partial\bar{F}_{TX}/\partial\bar{W}_X \cong -2C_{T\lambda}/(\overline{R\Omega}) \\ F_{TX,r} &= \partial\bar{F}_{TX}/\partial(br/V) \cong 0 \\ \bar{M}_{TZ,U_X} &= \partial\bar{M}_{TZ}/\partial\bar{U}_X \cong 0 \\ \bar{M}_{TZ,W_X} &= \partial\bar{M}_{TZ}/\partial\bar{W}_X \cong 0 \\ \bar{M}_{TZ,r} &= \partial\bar{M}_{TZ}/\partial(br/V) \cong (b/2V_B^{1/3})C_{T\lambda}/(\overline{R\Omega}) \end{aligned}\right\} \tag{3.9}$$

where

$$\overline{R\Omega} = (R\Omega)/\sqrt{V_B^{1/2}g}. \tag{3.10}$$

The above derivatives are also given in Table 3 for the present vehicle.

§4 Equations of Motion

A system consists of a vehicle and the surrounding fluid can be described by the Lagrange's equation of motion given by [4]

$$(d/dt)(\partial T/\partial\dot{q}_i) - \partial T/\partial q_i = Q_i \tag{4.1}$$

where T is the kinetic energy of the vehicle and the fluid, Q_i is the generalized force vector, and q_i is the generalized coordinate vector. The kinetic energy can be expressed as

$$T = (1/2)\sum_{i,j=1}^{6}(M_{ij}v_i v_j + A_{ij}v_i^w v_j^w) \tag{4.2}$$

where M_{ij} and A_{ij} are "generalized mass" and "added mass" respectively, and where v_i, v_j and v_i^w, v_j^w are components of the absolute velocity of vehicle, $\boldsymbol{U}$ and the relative velocity with respect to the surrounding fluid, $\boldsymbol{V}=\boldsymbol{U}-\boldsymbol{W}$, respectively or

$$\left.\begin{aligned} &v_1 = U_X, \quad v_2 = U_Y, \quad v_3 = U_Z \\ &v_1^w = U_X - W_X, \quad v_2^w = U_Y - W_Y, \quad v_3^w = U_Z - W_Z \\ &v_4 = v_4^w = \omega_X, \quad v_5 = v_5^w = \omega_Y, \quad v_6 = v_6^w = \omega_Z. \end{aligned}\right\} \tag{4.3}$$

The generalized mass is given by

$$\left.\begin{aligned} M_{ij} &= M\delta_{ij} && (\text{for } i, j = 1\sim3) \\ &= \varepsilon_{i(j-3)k}Mr_{G,k} && (\text{for } i,\ k = 1\sim3,\ j = 4\sim6) \\ &= -\varepsilon_{(i-3)jk}Mr_{G,k} && (\text{for } j,\ k = 1\sim3,\ i = 4\sim6) \\ &= (-1)^{1+\delta_{ij}}I_{ij} && (\text{for } i, j = 4\sim6) \end{aligned}\right\} \tag{4.4}$$

where ε_{ijk} is zero if any two of the indices i, j, k are alike and $+1$ or -1 according as the indices are in cyclic or anticyclic order, and where $M(=W/g)$, $r_{G,k}$ and I_{ij} are mass, center of gravity and moments of inertia $(i=j)$ or products of inertia $(i\neq j)$ respectively.

By using velocity potential components of a potential function Φ,

$$\Phi=\sum_{i=1}^{6} v_i^w \Phi_i, \tag{4.5}$$

the added mass can be expressed as [3]

$$A_{ij}=-\int \rho\Phi_i(\nabla\Phi_j)\cdot \boldsymbol{n}dS \tag{4.6}$$

where $\boldsymbol{n}dS$ is the normal component of an elemental surface of the vehicle and the integration should be extended over all external surface of the vehicle.

A summation of the generatized mass and the added mass is sometimes called "virtual mass". Since they are symmetric, there are 10 generalized masses and 21 added masses for a given body as shown in Table 5 and 6 respectively, in the latter of which only 15 are independent.

If the body of vehicle has a mirror symmetry about XZ plane like the present case, the following terms will vanish:

TABLE 5 Generalized mass

v_i \ v_j	1	2	3	4	5	6
1	M	0	0	0	Mz_G	$-My_G$
2	0	M	0	$-Mz_G$	0	Mx_G
3	0	0	M	My_G	$-Mx_G$	0
4	0	$-Mz_G$	My_G	I_{44}	$-I_{45}$	$-I_{46}$
5	Mz_G	0	$-Mx_G$	$-I_{45}$	I_{55}	$-I_{56}$
6	$-My_G$	Mx_G	0	$-I_{46}$	$-I_{56}$	I_{66}

TABLE 6 Added mass

v_i \ v_j	1	2	3	4	5	6
1	A_{11}	A_{12}	A_{13}	A_{14}	A_{15}	A_{16}
2	A_{12}	A_{22}	A_{23}	A_{24}	A_{25}	A_{26}
3	A_{13}	A_{23}	A_{33}	A_{34}	A_{35}	A_{36}
4	A_{14}	A_{24}	A_{34}	A_{44}	A_{45}	A_{46}
5	A_{15}	A_{25}	A_{35}	A_{45}	A_{55}	A_{56}
6	A_{16}	A_{26}	A_{36}	A_{46}	A_{56}	A_{66}

$$\left.\begin{aligned} &y_G = I_{45} = I_{56} = 0 \\ &A_{12} = A_{14} = A_{16} = A_{23} = A_{25} = A_{34} = A_{36} = A_{45} = A_{56} = 0. \end{aligned}\right\} \tag{4.7}$$

Now let q_i be vectorial components of the origin of the body coordinate system along (X_0, Y_0, Z_0) axes and orientation of the vehicle or Eulerian angles,

$$\left.\begin{aligned} &q_1 = X, \quad q_2 = Y, \quad q_3 = Z, \\ &q_4 = \phi, \quad q_5 = \theta, \quad q_6 = \psi. \end{aligned}\right\} \tag{4.8}$$

Thus, by using equations (1.2) and (1.3), the linear and angular velocities of the vehicle can be given as

$$v_i = \sum_r \alpha_{ir} \dot{q}_r \tag{4.9}$$

where

$$\left.\begin{aligned} \dot{q}_r &= (\dot{X}, \dot{Y}, \dot{Z}, \dot{\phi}, \dot{\theta}, \dot{\psi})^T \\ &= (U_{X_0}, U_{Y_0}, U_{Z_0}, \dot{\phi}, \dot{\theta}, \dot{\psi})^T \end{aligned}\right\} \tag{4.10}$$

and

$$\alpha_{ir} = \begin{pmatrix} T_B & 0 \\ 0 & \boldsymbol{T} \end{pmatrix}$$

$$\begin{bmatrix} \cos\theta\cos\psi & \cos\theta\sin\psi, & -\sin\theta & 0, & 0, & 0, \\ \cos\psi\sin\phi\sin\theta - \sin\psi\cos\phi & \sin\psi\sin\phi\sin\theta + \cos\psi\cos\phi & \sin\phi\cos\theta & 0, & 0, & 0, \\ \cos\psi\cos\phi\sin\theta + \sin\psi\sin\theta & \sin\psi\cos\phi\sin\theta - \cos\psi\sin\phi & \cos\theta\cos\phi, & 0, & 0, & 0, \\ 0, & 0, & 0, & 1, & 0, & -\sin\theta \\ 0, & 0, & 0, & 0, & \cos\phi, & \cos\theta\sin\phi \\ 0, & 0, & 0, & 0, & -\sin\phi, & \cos\theta\cos\phi \end{bmatrix} \tag{4.11}$$

By considering the kinetic energy as

$$T = T(q_r, \dot{q}_r; t) = T(v_i; t) \tag{4.12}$$

the first and the second terms in the left-hand side of Lagrange's equation become

$$\begin{aligned} (d/dt)(\partial T/\partial \dot{q}_r) &= (d/dt)\{(\partial T/\partial v_i)(\partial v_i/\partial \dot{q}_r)\} = (d/dt)(\partial T/\partial v_i)\alpha_{ir} + (\partial T/\partial v_i)\dot{\alpha}_{ir} \\ &= (d/dt)(\partial T/\partial v_i)\alpha_{ir} + (\partial T/\partial v_i)(\partial \alpha_{ir}/\partial q)\dot{q}_s \\ &= (d/dt)(\partial T/\partial v_i)\alpha_{ir} + (\partial T/\partial v_i)(\partial \alpha_{ir}/\partial q_s)\beta_{sk} v_k \end{aligned}$$

$$\begin{aligned} \partial T/\partial q_r &= (\partial T/\partial v)(\partial v_i/\partial q_r) = (\partial T/\partial v_i)(\partial \alpha_{is}/\partial q_r) q_s \\ &= (\partial T/\partial v_i)(\partial \alpha_{is}/\partial q_r)\beta_{sk} v_k. \end{aligned}$$

Then the original equation can be written as

$$(d/dt)(\partial T/\partial v_i)\alpha_{ir}+(\partial T/\partial v_i)(\partial\alpha_{ir}/\partial q_s)\beta_{sk}v_k-(\partial T/\partial v_i)(\partial\alpha_{is}/\partial q_r)\beta_{sk}v_k=Q_r$$

Operating an inverse matrix of α_{ir} or $\beta_{ri}=\alpha_{ri}^{-1}$ from the right-hand side yields

$$(d/dt)(\partial T/\partial v_i)+(\partial T/\partial v_j)\gamma_{ijk}v_k=\Pi_i \tag{4.13}$$

where

$$\left.\begin{aligned}\gamma_{ijk}&=\sum_{r,s}(\partial\alpha_{jr}/\partial q_s-\partial\alpha_{js}/\partial q_r)\beta_{sk}\beta_{ri}\\ \Pi_i&=\sum_{r}Q_r\beta_{ri}.\end{aligned}\right\} \tag{4.14}$$

Since the v_i, α_{ir} and β_{ri} can be written as

$$v_i=\begin{pmatrix}\boldsymbol{U}\\ \boldsymbol{\omega}\end{pmatrix}\quad \alpha_{ir}=\begin{pmatrix}\boldsymbol{T}_B, & 0\\ 0 & \boldsymbol{T}\end{pmatrix}\quad \beta_{ri}=\begin{pmatrix}\boldsymbol{T}_B^{-1}, & 0\\ 0 & \boldsymbol{T}^{-1}\end{pmatrix}$$

the second term in the left-hand side of equation (4.13) becomes

$$\left.\begin{aligned}(\partial T/\partial v_j)\gamma_{ijk}v_k&=\boldsymbol{\omega}\times(\partial T/\partial\boldsymbol{U}) && \text{for } i=1,2,3\\ &=\boldsymbol{U}\times(\partial T/\partial\boldsymbol{U})+\boldsymbol{\omega}\times(\partial T/\partial\boldsymbol{\omega}) && \text{for } i=4,5,6.\end{aligned}\right\}$$

Thus equation (4.13) yields

$$\left.\begin{aligned}&(d/dt)(\partial T/\partial\boldsymbol{U})+\boldsymbol{\omega}\times(\partial T/\partial\boldsymbol{U})=\boldsymbol{F}\\ &(d/dt)(\partial T/\partial\omega)+\boldsymbol{U}\times(\partial T/\partial\boldsymbol{U})+\boldsymbol{\omega}\times(\partial T/\partial\boldsymbol{\omega})=\boldsymbol{M}\end{aligned}\right\}$$

or

$$\left.\begin{aligned}&(d/dt)(\partial T/\partial U_X)-\omega_Z(\partial T/\partial U_Y)+\omega_Y(\partial T/\partial U_Z)=F_X\\ &(d/dt)(\partial T/\partial U_Y)-\omega_X(\partial T/\partial U_Z)+\omega_Z(\partial T/\partial U_X)=F_Y\\ &(d/dt)(\partial T/\partial U_Z)-\omega_Y(\partial T/\partial U_X)+\omega_X(\partial T/\partial U_Y)=F_Z\\ &(d/dt)(\partial T/\partial\omega_X)-U_Z(\partial T/\partial U_Y)+U_Y(\partial T/\partial U_Z)-\omega_Z(\partial T/\partial\omega_Y)+\omega_Y(\partial T/\partial\omega_Z)=M_X\\ &(d/dt)(\partial T/\partial\omega_Y)-U_X(\partial T/\partial U_Z)+U_Z(\partial T/\partial U_X)-\omega_X(\partial T/\partial\omega_Z)+\omega_Z(\partial T/\partial\omega_X)=M_Y\\ &(d/dt)(\partial T/\partial\omega_Z)-U_Y(\partial T/\partial U_X)+U_X(\partial T/\partial U_Y)+\omega_Y(\partial T/\partial\omega_X)-\omega_X(\partial T/\partial\omega_Y)=M_Z.\end{aligned}\right\} \tag{4.15}$$

The above expression of the equations of motion in the body-fixed-coordinate system can also be obtained by considering the "impulse" of the system [7].

By substituting equation (4.2) into the kinetic energy, T, and by nondimensionalyzing equation (4.15) the following equation of motion of the immersed vehicle about the origin of the body-fixed-coordinate system, (X, Y, Z), can be obtained:

$$\begin{pmatrix}\bar{F}_X\\ \bar{F}_Y\\ \bar{F}_Z\end{pmatrix}=\bar{M}\left\{\begin{pmatrix}\bar{U}'_X\\ \bar{U}'_Y\\ \bar{U}'_Z\end{pmatrix}+\begin{pmatrix}\bar{U}_Z\bar{\omega}_Y-\bar{U}_Y\bar{\omega}_Z\\ \bar{U}_X\bar{\omega}_Z-\bar{U}_Z\bar{\omega}_X\\ \bar{U}_Y\bar{\omega}_X-\bar{U}_X\bar{\omega}_Y\end{pmatrix}\right.$$

$$
\left.
\begin{aligned}
&+\begin{pmatrix}
-\bar{x}_G(\bar{\omega}_Y^2+\bar{\omega}_Z^2)-\bar{y}_G(\bar{\omega}'_Z-\bar{\omega}_X\bar{\omega}_Y)+\bar{z}_G(\bar{\omega}'_Y+\bar{\omega}_X\bar{\omega}_Z)\\
-\bar{y}_G(\bar{\omega}_Z^2+\bar{\omega}_X^2)-\bar{z}_G(\bar{\omega}'_X-\bar{\omega}_Y\bar{\omega}_Z)+\bar{x}_G(\bar{\omega}'_Z+\bar{\omega}_X\bar{\omega}_Y)\\
-\bar{z}_G(\bar{\omega}_X^2+\bar{\omega}_Y^2)-\bar{x}_G(\bar{\omega}'_Y-\bar{\omega}_X\bar{\omega}_Z)+\bar{y}_G(\bar{\omega}'_X+\bar{\omega}_Y\bar{\omega}_Z)
\end{pmatrix}\Bigg\}\\
&+\left\{\begin{pmatrix}
\bar{A}_{11}\bar{V}'_X+\bar{A}_{12}\bar{V}'_Y+\bar{A}_{13}\bar{V}'_Z+\bar{A}_{14}\bar{\omega}'_X+\bar{A}_{15}\bar{\omega}'_Y+\bar{A}_{16}\bar{\omega}'_Z\\
\bar{A}_{12}\bar{V}'_X+\bar{A}_{22}\bar{V}'_Y+\bar{A}_{23}\bar{V}'_Z+\bar{A}_{24}\bar{\omega}'_X+\bar{A}_{25}\bar{\omega}'_Y+\bar{A}_{26}\bar{\omega}'_Z\\
\bar{A}_{13}\bar{V}'_X+\bar{A}_{23}\bar{V}'_Y+\bar{A}_{33}\bar{V}'_Z+\bar{A}_{34}\bar{\omega}'_X+\bar{A}_{35}\bar{\omega}'_Y+\bar{A}_{36}\bar{\omega}'_Z
\end{pmatrix}\right.\\
&+\begin{pmatrix}
(\bar{A}_{13}\bar{V}_X+\bar{A}_{23}\bar{V}_Y+\bar{A}_{33}\bar{V}_Z+\bar{A}_{34}\bar{\omega}_X+\bar{A}_{35}\bar{\omega}_Y+\bar{A}_{36}\bar{\omega}_Z)\bar{\omega}_Y\\
(\bar{A}_{11}\bar{V}_X+\bar{A}_{12}\bar{V}_Y+\bar{A}_{13}\bar{V}_Z+\bar{A}_{14}\bar{\omega}_X+\bar{A}_{15}\bar{\omega}_Y+\bar{A}_{16}\bar{\omega}_Z)\bar{\omega}_Z\\
(\bar{A}_{12}\bar{V}_X+\bar{A}_{22}\bar{V}_Y+\bar{A}_{23}\bar{V}_Z+\bar{A}_{24}\bar{\omega}_X+\bar{A}_{25}\bar{\omega}_Y+\bar{A}_{26}\bar{\omega}_Z)\bar{\omega}_X
\end{pmatrix}\\
&\left.-\begin{pmatrix}
(\bar{A}_{12}\bar{V}_X+\bar{A}_{22}\bar{V}_Y+\bar{A}_{23}\bar{V}_Z+\bar{A}_{24}\bar{\omega}_X+\bar{A}_{25}\bar{\omega}_Y+\bar{A}_{26}\bar{\omega}_Z)\bar{\omega}_Z\\
(\bar{A}_{13}\bar{V}_X+\bar{A}_{23}\bar{V}_Y+\bar{A}_{33}\bar{V}_Z+\bar{A}_{34}\bar{\omega}_X+\bar{A}_{35}\bar{\omega}_Y+\bar{A}_{36}\bar{\omega}_Z)\bar{\omega}_X\\
(\bar{A}_{11}\bar{V}_X+\bar{A}_{12}\bar{V}_Y+\bar{A}_{13}\bar{V}_Z+\bar{A}_{14}\bar{\omega}_X+\bar{A}_{15}\bar{\omega}_Y+\bar{A}_{16}\bar{\omega}_Z)\bar{\omega}_Y
\end{pmatrix}\right\}
\end{aligned}
\right\}
\quad (4.16)
$$

$$
\left.
\begin{aligned}
\begin{pmatrix}\bar{M}_X\\ \bar{M}_Y\\ \bar{M}_Z\end{pmatrix}
&=\left\{\begin{pmatrix}
\bar{I}_X\bar{\omega}'_X-\bar{J}_{XY}\bar{\omega}'_Y-\bar{J}_{XZ}\bar{\omega}'_Z\\
\bar{I}_Y\bar{\omega}'_Y-\bar{J}_{YZ}\bar{\omega}'_Z-\bar{J}_{XY}\bar{\omega}'_X\\
\bar{I}_Z\bar{\omega}'_Z-\bar{J}_{XZ}\bar{\omega}'_X-\bar{J}_{YZ}\bar{\omega}'_Y
\end{pmatrix}\right.
+\begin{pmatrix}
(\bar{I}_Z-\bar{I}_Y)\bar{\omega}_Y\bar{\omega}_Z\\
(\bar{I}_X-\bar{I}_Z)\bar{\omega}_X\bar{\omega}_Z\\
(\bar{I}_Y-\bar{I}_X)\bar{\omega}_X\bar{\omega}_Y
\end{pmatrix}\\
&+\begin{pmatrix}
(\bar{J}_{XY}\bar{\omega}_X+\bar{J}_{YZ}\bar{\omega}_Z)\bar{\omega}_Z-(\bar{J}_{XZ}\bar{\omega}_X+\bar{J}_{YZ}\bar{\omega}_Y)\bar{\omega}_Y\\
(\bar{J}_{YZ}\bar{\omega}_Y+\bar{J}_{XZ}\bar{\omega}_X)\bar{\omega}_X-(\bar{J}_{XY}\bar{\omega}_Y+\bar{J}_{XZ}\bar{\omega}_Z)\bar{\omega}_Z\\
(\bar{J}_{XZ}\bar{\omega}_Z+\bar{J}_{XY}\bar{\omega}_Y)\bar{\omega}_Y-(\bar{J}_{YZ}\bar{\omega}_Z+\bar{J}_{XY}\bar{\omega}_X)\bar{\omega}_X
\end{pmatrix}\\
&\left.+M\begin{pmatrix}
\bar{y}_G(\bar{U}'_Z+U_Y\omega_X-\bar{U}_X\bar{\omega}_Y)-\bar{z}_G(\bar{U}'_Y-U_Z\omega_X+\bar{U}_X\bar{\omega}_Z)\\
\bar{z}_G(\bar{U}'_X+U_Z\omega_Y-\bar{U}_Y\bar{\omega}_Z)-\bar{x}_G(\bar{U}'_Z-U_X\omega_Y+\bar{U}_Y\bar{\omega}_X)\\
\bar{x}_G(\bar{U}'_Y+U_X\omega_Z-\bar{U}_Z\bar{\omega}_X)-\bar{y}_G(\bar{U}'_X-U_Y\omega_Z+\bar{U}_Z\bar{\omega}_Y)
\end{pmatrix}\right\}\\
&+\left\{\begin{pmatrix}
\bar{A}_{14}\bar{V}'_X+\bar{A}_{24}\bar{V}_Y+\bar{A}_{34}\bar{V}_Z+\bar{A}_{44}\bar{\omega}_X+\bar{A}_{45}\bar{\omega}_Y+\bar{A}_{46}\bar{\omega}_Z\\
\bar{A}_{15}\bar{V}'_X+\bar{A}_{25}\bar{V}_Y+\bar{A}_{35}\bar{V}_Z+\bar{A}_{45}\bar{\omega}_X+\bar{A}_{55}\bar{\omega}_Y+\bar{A}_{56}\bar{\omega}_Z\\
\bar{A}_{16}\bar{V}'_X+\bar{A}_{26}\bar{V}_Y+\bar{A}_{36}\bar{V}_Z+\bar{A}_{45}\bar{\omega}_X+\bar{A}_{56}\bar{\omega}_Y+\bar{A}_{66}\bar{\omega}_Z
\end{pmatrix}\right.\\
&+\begin{pmatrix}
(\bar{A}_{13}\bar{V}_X+\bar{A}_{23}\bar{V}_Y+\bar{A}_{33}\bar{V}_Z+\bar{A}_{34}\bar{\omega}_X+\bar{A}_{35}\bar{\omega}_Y+\bar{A}_{36}\bar{\omega}_Z)\bar{V}_Y\\
(\bar{A}_{11}\bar{V}_X+\bar{A}_{12}\bar{V}_Y+\bar{A}_{13}\bar{V}_Z+\bar{A}_{14}\bar{\omega}_X+\bar{A}_{15}\bar{\omega}_Y+\bar{A}_{16}\bar{\omega}_Z)\bar{V}_Z\\
(\bar{A}_{12}\bar{V}_X+\bar{A}_{22}\bar{V}_Y+\bar{A}_{23}\bar{V}_Z+\bar{A}_{24}\bar{\omega}_X+\bar{A}_{25}\bar{\omega}_Y+\bar{A}_{26}\bar{\omega}_Z)\bar{V}_X
\end{pmatrix}\\
&-\begin{pmatrix}
(\bar{A}_{12}\bar{V}_X+\bar{A}_{22}\bar{V}_Y+\bar{A}_{23}\bar{V}_Z+\bar{A}_{24}\bar{\omega}_X+\bar{A}_{25}\bar{\omega}_Y+\bar{A}_{26}\bar{\omega}_Z)\bar{V}_Z\\
(\bar{A}_{13}\bar{V}_X+\bar{A}_{23}\bar{V}_Y+\bar{A}_{33}\bar{V}_Z+\bar{A}_{34}\bar{\omega}_X+\bar{A}_{35}\bar{\omega}_Y+\bar{A}_{36}\bar{\omega}_Z)\bar{V}_X\\
(\bar{A}_{11}\bar{V}_X+\bar{A}_{12}\bar{V}_Y+\bar{A}_{13}\bar{V}_Z+\bar{A}_{14}\bar{\omega}_X+\bar{A}_{15}\bar{\omega}_Y+\bar{A}_{16}\bar{\omega}_Z)\bar{V}_Y
\end{pmatrix}\\
&+\begin{pmatrix}
(\bar{A}_{16}\bar{V}_X+\bar{A}_{26}\bar{V}_Y+\bar{A}_{36}\bar{V}_Z+\bar{A}_{46}\bar{\omega}_X+\bar{A}_{56}\bar{\omega}_Y+\bar{A}_{66}\bar{\omega}_Z)\bar{\omega}_Y\\
(\bar{A}_{14}\bar{V}_X+\bar{A}_{24}\bar{V}_Y+\bar{A}_{34}\bar{V}_Z+\bar{A}_{44}\bar{\omega}_X+\bar{A}_{45}\bar{\omega}_Y+\bar{A}_{46}\bar{\omega}_Z)\bar{\omega}_Z\\
(\bar{A}_{15}\bar{V}_X+\bar{A}_{25}\bar{V}_Y+\bar{A}_{35}\bar{V}_Z+\bar{A}_{45}\bar{\omega}_X+\bar{A}_{55}\bar{\omega}_Y+\bar{A}_{56}\bar{\omega}_Z)\bar{\omega}_X
\end{pmatrix}\\
&\left.-\begin{pmatrix}
(\bar{A}_{15}\bar{V}_X+\bar{A}_{25}\bar{V}_Y+\bar{A}_{35}\bar{V}_Z+\bar{A}_{45}\bar{\omega}_X+\bar{A}_{55}\bar{\omega}_Y+\bar{A}_{56}\bar{\omega}_Z)\bar{\omega}_Z\\
(\bar{A}_{16}\bar{V}_X+\bar{A}_{26}\bar{V}_Y+\bar{A}_{36}\bar{V}_Z+\bar{A}_{46}\bar{\omega}_X+\bar{A}_{56}\bar{\omega}_Y+\bar{A}_{66}\bar{\omega}_Z)\bar{\omega}_X\\
(\bar{A}_{14}\bar{V}_X+\bar{A}_{24}\bar{V}_Y+\bar{A}_{34}\bar{V}_Z+\bar{A}_{44}\bar{\omega}_X+\bar{A}_{45}\bar{\omega}_Y+\bar{A}_{46}\bar{\omega}_Z)\bar{\omega}_Y
\end{pmatrix}\right\}.
\end{aligned}
\right\}
\quad (4.17)
$$

where

$$\left.\begin{aligned}(\bar{F}_X, \bar{F}_Y, \bar{F}_Z)&=(F_X, F_Y, F_Z)/\rho g V_B\\ (\bar{M}_X, \bar{M}_Y, \bar{M}_Z)&=(M_X, M_Y, M_Z)/\rho g V_B^{4/3}\end{aligned}\right\} \tag{4.18}$$

$$\left.\begin{aligned}\bar{M}&=M/\rho V_B=\rho_B/\rho\\ (\bar{I}_X, \bar{I}_Y, \bar{I}_Z)&=(I_{44}, I_{55}, I_{66})/\rho V_B^{5/3}\\ (\bar{J}_{XY}, \bar{J}_{XZ}, \bar{J}_{YZ})&=(I_{45}, I_{46}, I_{56})/\rho V_B^{5/3}\end{aligned}\right\} \tag{4.19}$$

$$(\bar{x}_G, \bar{y}_G, \bar{z}_G)=(x_G, y_G, z_G)/V_B^{1/3} \tag{4.20}$$

$$\left.\begin{aligned}(\bar{U}_X, \bar{U}_Y, \bar{U}_Z)&=(U_X, U_Y, U_Z)/\sqrt{V_B^{1/3}g}\\ (\bar{V}_X, \bar{V}_Y, \bar{V}_Z)&=(V_X, V_Y, V_Z)/\sqrt{V_B^{1/3}g}\end{aligned}\right\} \tag{4.21}$$

$$(\bar{\omega}_X, \bar{\omega}_Y, \bar{\omega}_Z)=(\omega_X, \omega_Y, \omega_Z)/\sqrt{g/V_B^{1/3}}$$

$$\left.\begin{aligned}&\bar{A}_{ij}=A_{ij}/\rho V_B && \text{for } i, j\leq 3\\ &\bar{A}_{ij}=A_{ij}/\rho V_B^{4/3} && \text{for } i\leq 3 \text{ and } j\geq 4\\ & && \text{or } j\leq 3 \text{ and } i\geq 4\\ &\bar{A}_{ij}=A_{ij}/\rho V_B^{5/3} && \text{for } i, j\geq 4\end{aligned}\right\} \tag{4.23}$$

$$\left.\begin{aligned}&\bar{t}=t/\sqrt{V_B^{1/3}/g}\\ &(\ \ )'=\partial(\ \ )/\partial\bar{t}=(\ \cdot\ )\sqrt{V_B^{1/3}/g}.\end{aligned}\right\} \tag{4.24}$$

The first bracket in each of the above equations shows the inertia terms related to the body itself and the second bracket shows those related to the fluid due to the added masses. It must be remembered that the added mass effects are related to the relative fluid velocity, V, instead of the absolute velocity, $\boldsymbol{U}$.

Substituting the results obtained in the preceding sections, §2 and §3, into the left hand side of equations (4.16) and (4.17) the detailed expression of the non-dimensional external forces and moments can be given as follows:

$$\begin{pmatrix}\bar{F}_X\\ \bar{F}_Y\\ \bar{F}_Z\end{pmatrix}=(1-\bar{M})\begin{pmatrix}\sin\theta\\ -\cos\theta\sin\phi\\ -\cos\theta\cos\phi\end{pmatrix}+F_r\begin{pmatrix}C_{FX}\\ C_{FY}\\ C_{FZ}\end{pmatrix}+P\begin{pmatrix}\bar{F}_{TX}\\ 0\\ 0\end{pmatrix} \tag{4.25}$$

$$\left.\begin{aligned}\begin{pmatrix}\bar{M}_X\\ \bar{M}_Y\\ \bar{M}_Z\end{pmatrix}&=\begin{pmatrix}(\bar{y}_B-\bar{M}y_G)\cos\theta\cos\phi++(\bar{z}_B-\bar{M}\bar{z}_G)\cos\phi\sin\phi\\ (\bar{z}_B-\bar{M}\bar{z}_G)\sin\theta+(\bar{x}_B-\bar{M}\bar{x}_G)\cos\theta\cos\phi\\ -(\bar{x}_B-\bar{M}\bar{x}_G)\cos\theta\sin\phi-(\bar{y}_B-\bar{M}\bar{y}_G)\sin\theta\end{pmatrix}\\ &\quad+F_r\begin{pmatrix}C_{MX}\\ C_{MY}\\ C_{MZ}\end{pmatrix}+P\begin{pmatrix}0\\ 0\\ \bar{M}_{TZ}\end{pmatrix}\end{aligned}\right\} \tag{4.26}$$

where

$$(\bar{x}_B, \bar{y}_B, \bar{z}_B) = (x_B, y_B, z_B)/V_B^{1/3} \tag{4.27}$$

$$\left.\begin{aligned} F_r &= (1/2)\rho V^2 V_B^{2/3}/\rho g V_B = (1/2)\{(U/\sqrt{gV_B^{1/3}}) - (W/\sqrt{gV_B^{1/3}})\}^2 \\ &= (1/2)(\bar{U} - \bar{W})^2 \end{aligned}\right\} \tag{4.28}$$

$$P = \rho S(R\Omega)^2/\rho g V_B = (S/V_B^{2/3})(R\Omega/\sqrt{gV_B^{1/3}}) = (S/V_B^{2/3})\overline{R\Omega} \tag{4.29}$$

and where either F_r itself or sometmes, $\sqrt{2F_r}$ is called "Froud number".

All necessary dimensional and nondimensional quantities related to the body of the present vehicle are listed in Table 7.

TABLE 7 Dimensional and nondimensional values of necessary parameters.

Items		Definite	Dimensional value	Nondimensional value
Reference values	Time	$\sqrt{V_B^{1/3}/g}$	0.3935 sec	2.5414 for 1 sec
	Distance	$V_B^{1/3}$	1.5173 m	0.6591 for 1 m
	Velocity	$\sqrt{V_B g}$	3.8561 m/sec	0.2593 for 1 m/sec²
	Acceleration	g	9.8 m/sec²	0.10204 for 1 m/sec²
	Force	$\rho g V_B$	3,577.2 kg	2.795×10^{-4} for 1 kg
	Moment	$\rho g V_B^{4/3}$	5,427.7 kg·m	1.842×10^{-3} for 1 kg·m
	Mass	ρV_B	365.02 kgsec²/m	2.740×10^{-3} for 1 kgsec²/m
	Mass moment	$\rho V_B^{4/3}$	553.84 kgsec²	1.8055×10^{-3} for 1 kgsec²
	Moment of inertia	ρV_B	840.31 kgsec²m	1.190×10^{-3} for 1 kgsec²m
	Angular velocity	$\sqrt{g/V_B}$	2.5414 rad/sec	0.3935 for 1 rad/sec
	Angular acceleration	g/V_B	6.4588 rad/sec	0.1548 for 1 rad/sec²
Center of gravity		$x_{G,0}$	0 m	0
		$y_{G,0}$	0 m	0
		$z_{G,0}$	0.038 m	0.0250
Center of buoyancy		$x_{B,0}$	0 m	0
		$y_{B,0}$	0 m	0
		$z_{B,0}$	−0.0030 m	−0.00198
Location of thrusters		x_T	0.391 m	0.258
		$y_T(=b/2)$	±0.90 m	±0.593
		z_T	0.04 m	0.0264
Mass		M	365±4.1	1.00±0.011
Moment of intertia		I_X	60.4 kg·msec²	0.0719
		I_Y	504.9 kg·msec²	0.6008
		I_Z	488.4 kg·msec²	0.5812
		J_{XZ}	9.5 kg·msec²	0.0113
Maximum buoyant force		B_0	3,834 kg	1.072

§5 TRIMMED STATE

If the vehicle is considered to be in a steady flight (either straight or turning

$\omega_Z \neq 0$) and if the $\bar{y}_G$ and $\bar{y}_B$ are zero, then the all unsteady inertial terms will be discarded in equations (4.16) and (4.17) and the following trimmed equations can be derived:

$$\left.\begin{aligned} &\bar{M}\left\{\begin{pmatrix} -\bar{U}_Y\bar{\omega}_Z \\ \bar{U}_X\bar{\omega}_Z \\ 0 \end{pmatrix} + \begin{pmatrix} -x_G\bar{\omega}_Z^2 \\ 0 \\ 0 \end{pmatrix}\right\} + \begin{pmatrix} (\bar{A}_{22}\bar{U}_Y + \bar{A}_{26}\bar{\omega}_Z)\bar{\omega}_Z \\ (\bar{A}_{22}\bar{U}_X + \bar{A}_{13}\bar{U}_Z)\bar{\omega}_Z \\ 0 \end{pmatrix} \\ &= (1-\bar{M})\begin{pmatrix} \sin\theta \\ -\cos\theta\sin\phi \\ -\cos\theta\cos\phi \end{pmatrix} + F_r\begin{pmatrix} C_{F_X} \\ C_{F_Y} \\ C_{F_Z} \end{pmatrix} + P\begin{pmatrix} \bar{F}_{T_X} \\ 0 \\ 0 \end{pmatrix} \end{aligned}\right\} \qquad (5.1)$$

$$\left.\begin{aligned} &\begin{pmatrix} 0 \\ -\bar{J}_{XY}\bar{\omega}_Z^2 \\ 0 \end{pmatrix} + \bar{M}\begin{pmatrix} -\bar{z}_G\bar{U}_Y\bar{\omega}_Z \\ -\bar{z}_G\bar{U}_Y\bar{\omega}_Z \\ \bar{x}_G\bar{U}_X\bar{\omega}_Z \end{pmatrix} + \begin{pmatrix} (\bar{A}_{13}\bar{U}_X + \bar{A}_{33}\bar{U}_Z)\bar{U}_Y \\ (\bar{A}_{11}\bar{U}_X + \bar{A}_{13}\bar{U}_Z)\bar{U}_Z \\ (\bar{A}_{22}\bar{U}_Y + \bar{A}_{26}\bar{\omega}_Z)\bar{U}_X \end{pmatrix} \\ &-\begin{pmatrix} (\bar{A}_{15}\bar{U}_X + \bar{A}_{35}\bar{U}_Z)\bar{\omega}_Z \\ 0 \\ 0 \end{pmatrix} = \begin{pmatrix} (\bar{z}_B - \bar{M}\bar{z}_G)\cos\theta\sin\phi \\ (\bar{z}_B - \bar{M}\bar{z}_G)\sin\theta + \{\bar{x}_B - \bar{M}\bar{x}_G\}\cos\theta\cos\phi \\ -(\bar{x}_B - \bar{M}\bar{x}_G)\cos\theta\sin\phi \end{pmatrix} \\ &+ F_r\begin{pmatrix} C_{M_X} \\ C_{M_Y} \\ C_{M_Z} \end{pmatrix} + P\begin{pmatrix} 0 \\ 0 \\ \bar{M}_{T_Z} \end{pmatrix}. \end{aligned}\right\} \qquad (5.2)$$

(i) Steady Straight Flight

Since for the mirror symmetric body the C_{F_Y} and C_{M_X} are zero in steady straight motion in which no yawing control is applied or $\bar{M}_{T_Z}=0$ the rolling angle will be zero or $\phi=0$. Thus the second equation in equations (5.1) and the first and third equations in equations (5.2) may be discarded. The remained equations are as follows:

$$\left.\begin{aligned} &(1-\bar{M})\sin\theta + F_r C_{F_X} \pm P\bar{F}_{T_X} = 0 \\ &-(1-\bar{M})\cos\theta + F_r C_{F_Z} = 0 \\ &(\bar{z}_B - \bar{M}\bar{z}_G)\sin\theta + (\bar{x}_B - \bar{M}\bar{x}_G)\cos\theta + F_r C_{M_Y} = 0. \end{aligned}\right\} \qquad (5.3)$$

Fig. 8 shows trimmed states of the exemplified vehicle in terms of angle of attack α and of pitching angle θ, for various speeds or Froud numbers F_r, thrust $P\bar{F}_{T_X}$, vehicle's weight and center of gravity in water, $\bar{F}_B - \bar{W}$ and $\bar{x}_B - (\rho_B/\rho)\bar{x}_G$ respectively. The upper part of the respective figure gives the forward motion, while the lower part shows the backward motion.

In low forward speed the pitching angle is mainly decided by the horizontal location of the center of gravity and is less sensitive to the angle of attack of the vehicle because of low contribution of the hydrodynamic forces and moments. In high forward speed and in all backward speeds, the pitching angle is strongly related to both the horizontal location of the center of gravity and the angle of

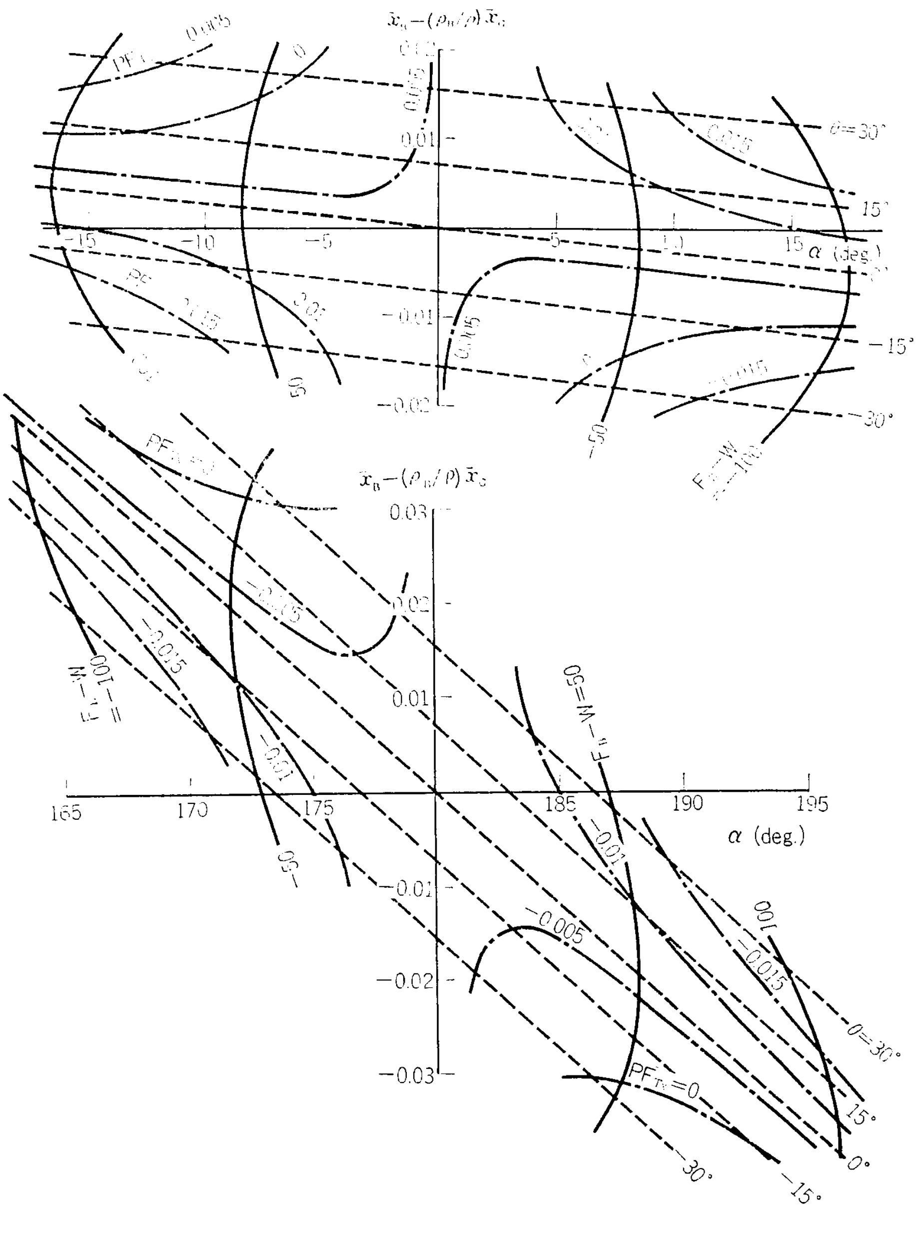

FIG. 8. Trimmed states of a submersible
(a) $F_r=0.05$

attack which is principally a function of the weight of the vehicle in water and the thrust. The positive angle of attack is resulted from the descending flight, whereas the negative angle of attack can be obtained by the ascending flight. It is interesting to find that the operational range of the angle of attack is reduced by increasing the Froud number or speed.

In hovering state in calm water or $\bar{F}_{T_x}=\bar{U}=\bar{W}=F_r=0$ the above equations require that

$$\bar{M}=1 \quad \text{or} \quad \rho_B=\rho \tag{5.4}$$

and

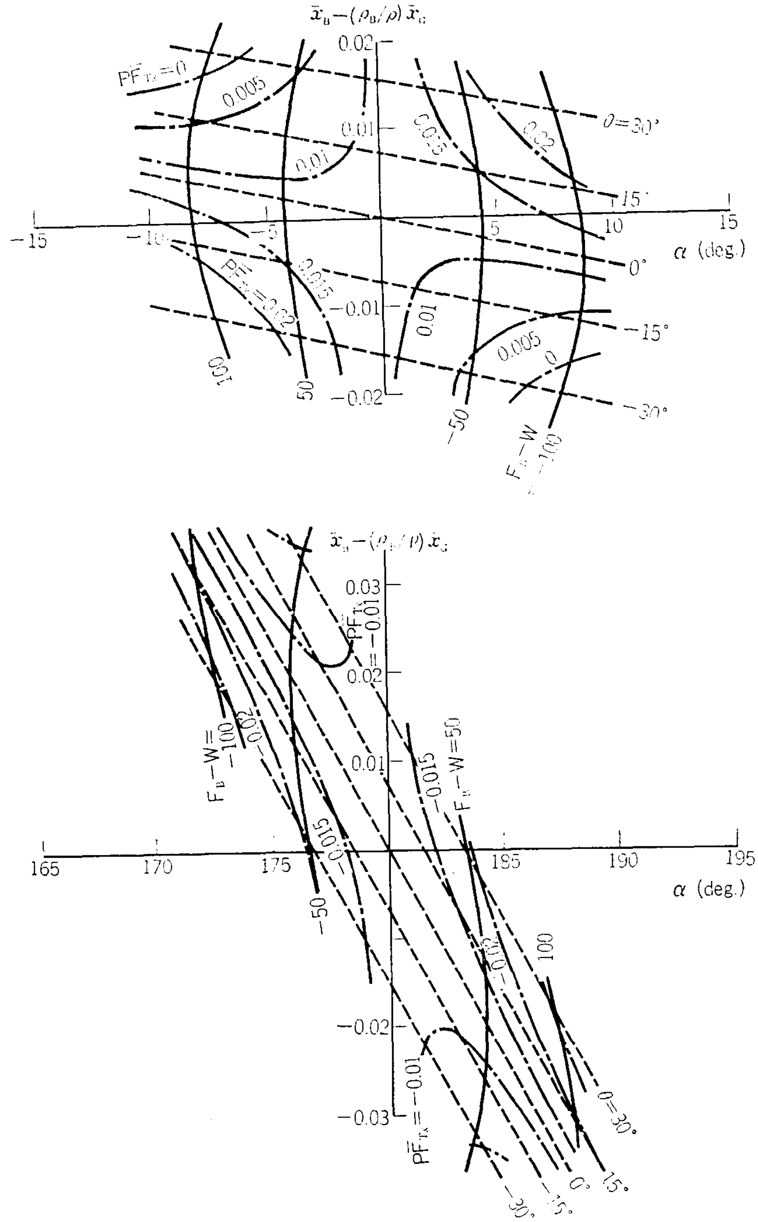

(b) $F_r=0.10$

$$\theta=\tan^{-1}\{(\bar{x}_B-\bar{x}_G)/(\bar{z}_G-\bar{z}_B)\} \tag{5.5}$$

where, different from surface vessels, the condition $\bar{z}_G \geq \bar{z}_B$ has been usually established. It will be appreciated that the mean density of the vehicle must be equal to that of the surrounding fluid in hovering flight and that the attitude of the vehicle will be determined by a ratio of the longitudinal and vertical distances between the center of buoyancy and the center of gravity.

(ii) Steady Turning Flight

The turn is, as stated in §3, conducted by operating the differential thruster drive. Then the equations of motion governed by this motion can be expressed as

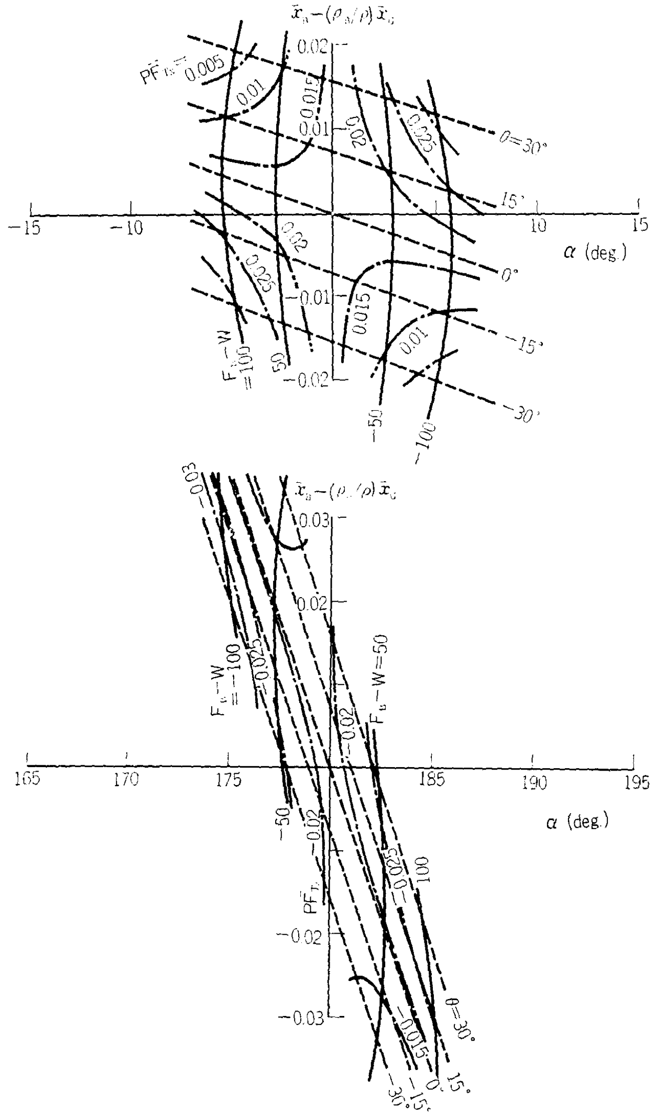

(c) $F_r=0.15$

$$
\left.
\begin{aligned}
&(-\bar{M}+\bar{A}_{22})\bar{U}_Y\bar{\omega}_Z+(-\bar{M}\bar{x}_G+\bar{A}_{26})\bar{\omega}_Z^2=(1-\bar{M})\sin\theta_0+F_rC_{F_X}+P\bar{F}_{T_X}\\
&(\bar{M}\bar{U}_X+\bar{A}_{11}\bar{U}_X+\bar{A}_{13}\bar{U}_Z)\bar{\omega}_Z=-(1-\bar{M})\cos\theta_0\sin\phi+F_rC_{F_Y}\\
&\{(-\bar{M}\bar{z}_G+\bar{A}_{15})\bar{U}_X-\bar{A}_{35}\bar{U}_Z\}\bar{\omega}_Z+(\bar{A}_{13}\bar{U}_X+\bar{A}_{33}\bar{U}_Z)\bar{U}_Y\\
&\quad=(\bar{z}_B-\bar{M}\bar{z}_G)\cos\theta_0\sin\phi+F_rC_{M_X}\\
&\bar{M}\bar{x}_G\bar{U}_X\bar{\omega}_Z+(\bar{A}_{22}\bar{U}_Y+\bar{A}_{26}\bar{\omega}_Z)\bar{U}_X=-(\bar{x}_B-\bar{M}\bar{x}_G)\cos\theta_0\sin\phi+F_rC_{M_Z}\pm\bar{M}_{T_Z}
\end{aligned}
\right\}
\quad (5.6)
$$

where unknown variables are $\bar{U}_X, \bar{U}_Y, \bar{\omega}_Z(=\bar{r})$, and ϕ, and where θ is assumed to be given as $\theta=\theta_0$.

The first equation will determine the Froud number,

$$
F_r=[(\bar{M}+\bar{A}_{22})\bar{U}_Y\bar{r}+(-\bar{M}\bar{x}_G+\bar{A}_{26})\bar{r}^2-(1-\bar{M})\sin\theta_0-P\bar{F}_{T_X}]/C_{F_X}, \quad (5.7)
$$

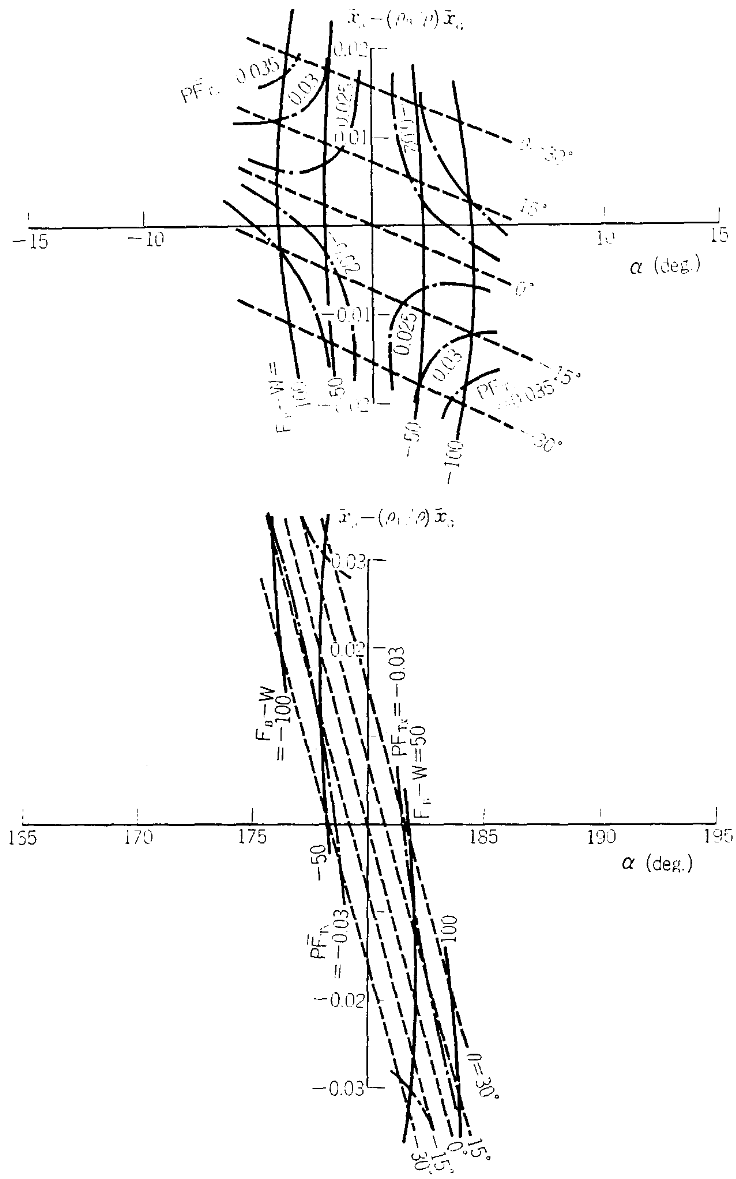

(d) $F_r=0.20$

which also gives the speed of the vehicle as approximately shown by

$$\bar{U}_X \cong 2[-(1-\bar{M})\sin\theta_0 - P\bar{F}_{T_X}]/C_{F_X,0} \tag{5.8}$$

where

$$C_{F_X,0} \cong -C_{D_0}.$$

The last equation will decide the turning rate which may be approximated by

$$\bar{M}\bar{x}_G\bar{U}_X\bar{\omega}_Z = F_r\bar{C}_{M_Z} \pm \bar{M}_{T_Z}$$

or

$$\left.\begin{aligned}\bar{M}\bar{x}_G\bar{U}_X\bar{\omega}_Z &= F_r\{C_{M_{Z,\beta}}(\bar{U}_Y/\bar{U}_0)+C_{M_{Z,r}}(\bar{r}/\bar{U}_0)\}\\ &\quad \pm P(b/2V_B^{1/3})\{C_{T_0}(1+\eta_T)+C_{T_\lambda}(\bar{v}_F+\bar{v}_B\pm\bar{b}\bar{r})/(\bar{R}\bar{\Omega})\}.\end{aligned}\right\} \quad (5.9)$$

Thus the rate $\bar{r}$ can be given by

$$\left.\begin{aligned}\bar{r} &= [\mp P(b/2V_B^{1/3})\{C_{T_0}(1+\eta_T)+C_{T_\lambda}(\bar{v}_F+\bar{v}_B)/\bar{R}\bar{\Omega}\}-C_{M_{Z,\beta}}(\bar{U}_Y/\bar{U}_0)]/\\ &\quad \{(C_{M_{Z,r}}/\bar{U}_0)+C_{T_\lambda}(\bar{b}/\bar{R}\bar{\Omega})-(\bar{M}\bar{x}_G\bar{U}_X/F_r)\}\\ &\cong \mp P(b/2V_B^{1/3})C_{T_0}(1+\eta_T)/\{(C_{M_{Z,r}}/\bar{U}_X)+C_{T_\lambda}(\bar{b}/\bar{R}\bar{\Omega})\}.\end{aligned}\right\} \quad (5.10)$$

The third equation will specify mainly the trimmed rolling angle of the vehicle as follows:

$$\left.\begin{aligned}\phi &= \sin^{-1}\{[\{(-\bar{M}\bar{z}_G+\bar{A}_{15})\bar{U}_X-\bar{A}_{35}\bar{U}_Z\}\bar{r}\\ &\quad +(\bar{A}_{13}\bar{U}_X+\bar{A}_{33}\bar{U}_Z)\bar{U}_Y-F_rC_{M_X}]/(\bar{z}_B-\bar{M}\bar{z}_G)\cos\theta_0\}\\ &\cong [(-M\bar{z}_G+\bar{A}_{15})\bar{U}_X\bar{r}-F_r\{C_{M_{X,r}}(\bar{r}/\bar{U}_X)\}]/(\bar{z}_B-\bar{M}\bar{z}_G)\cos\theta_0.\end{aligned}\right\} \quad (5.11)$$

Then the second equation will give the side slip angle, β, or the side velocity, $\bar{U}_Y$, as follows:

$$\left.\begin{aligned}\beta &= \sin^{-1}(\bar{U}_Y/\bar{U}_0)=[(\bar{M}\bar{U}_X+\bar{A}_{11}\bar{U}_X+\bar{A}_{13}\bar{U}_Z)\bar{\omega}_Z+(1-\bar{M})\cos\theta_0\sin\phi\\ &\quad -F_rC_{F_{Y,r}}(\bar{r}/\bar{U}_0)]/F_rC_{F_{Y,\beta}}\\ &\cong \bar{U}_Y/\bar{U}_X\cong[(\bar{M}+\bar{A}_{11})\bar{U}_X\bar{r}+(1-\bar{M})\cos\theta_0\sin\phi-F_rC_{F_{Y,r}}(\bar{r}/\bar{U}_0)]/F_rC_{F_{Y,\beta}}\end{aligned}\right\} \quad (5.12)$$

where $\bar{U}_X, \bar{r}$ and ϕ have been specified approximately by equations (5.8), (5.10) and (5.11) respectively.

When the vehicle is required to make "coordinated turn" which is a steady trimmed turn without side slip, $\dot{U}_Y=U_Y=0$, the rolling angle must be determined to satisfy the following condition:

$$\phi=\sin^{-1}[\{(\bar{M}+\bar{A}_{11})\bar{U}_X-F_rC_{F_{Y,r}}/\bar{U}_0\}\bar{r}/(\bar{M}-1)\cos\theta_0]. \quad (5.13)$$

Then the center of gravity will be specified to coincide equation (5.11) with equation (5.13). For completely balanced vehicle in buoyancy, or $\bar{M}=1$, the side slip will be cancelled if the $C_{F_{Y,r}}$ can be selected as

$$C_{F_{Y,r}}=(\bar{M}+\bar{A}_{11})\bar{U}_X\bar{U}_0/F_r. \quad (5.14)$$

The radius of turning, R, will be given by

$$R=\{\bar{U}_0/(\beta'+\bar{r})\}V_B^{1/3}\cong(\bar{U}_0/\bar{r})V_B^{1/3} \quad (5.15)$$

§6 Dynamic Characteristics

In order to simplify the analysis it will be assumed that the vehicle is flying in a current and is slightly disturbed from a steady-state equilibrium attitude and velocity, where the perturbed quantities are given as follows:

$$\left.\begin{aligned}&\bar{V}_X=\bar{V}_{X,0}+\Delta\bar{V}_X=(\bar{U}_{X,0}-\bar{W}_{X,0})+(\Delta\bar{U}_X-{}_X\bar{W}_X)\\&\bar{V}_Y=(\Delta\bar{U}_Y-\Delta\bar{W}_Y)\\&\bar{V}_Z=\bar{V}_{Z,0}+\Delta\bar{V}_Z=(\bar{U}_{Z,0}-\bar{W}_{Z,0})+(\Delta\bar{U}_Z-\Delta\bar{W}_Z)\end{aligned}\right\}\qquad(6.1)$$

$$\left.\begin{aligned}&\sin\psi=\Delta\psi,\qquad\cos\psi=1\\&\theta=\theta_0+\Delta\theta\\&\sin\phi=\Delta\phi,\qquad\cos\phi=1\end{aligned}\right\}\qquad(6.2)$$

$$\left.\begin{aligned}&\bar{\omega}_X=\phi'-\psi'\sin\theta_0\\&\bar{\omega}_Y=\theta'\\&\bar{\omega}_Z=\psi'\cos\theta_0\end{aligned}\right\}\qquad(6.3)$$

$$\left.\begin{aligned}&\bar{W}_{X,0}=(\bar{W}_{X_E,0}\cos\Psi+\bar{W}_{Y_E,0}\sin\Psi)\cos\theta_0-\bar{W}_{Z_E,0}\sin\theta_0\\&\bar{W}_{X,0}=-\bar{W}_{X_E,0}\sin\Psi+\bar{W}_{Y_E,0}\cos\Psi\\&\bar{W}_{Z,0}=(\bar{W}_{X_E,0}\cos\Psi+\bar{W}_{Y_E,0}\sin\Psi)\sin\theta_0+\bar{W}_{Z_E,0}\cos\theta_0\end{aligned}\right\}\qquad(6.4)$$

$$\left.\begin{aligned}&\Delta\bar{W}_X=(\Delta\bar{W}_{X_E}\cos\Psi+\bar{W}_{Y_E}\sin\Psi)\cos\theta_0-\bar{W}_{Z_E}\sin\theta_0-W_{Z,0}\Delta\theta\\&\Delta\bar{W}_Y=-\Delta W_{X_E}\sin\Psi+\Delta\bar{W}_{Y_E}\cos\Psi-(\bar{W}_{X_{E,0}}\cos\Psi+\bar{W}_{Y_{E,0}}\sin\Psi)\Delta\psi+\bar{W}_{Z,0}\Delta\phi\\&\Delta\bar{W}_Z=(\Delta\bar{W}_{X_E}\cos\Psi+\Delta\bar{W}_{Y_E}\sin\Psi)\sin\theta_0+\Delta\bar{W}_{Z_E}\cos\theta_0+\bar{W}_{X,0}\Delta\theta\end{aligned}\right\}\qquad(6.5)$$

$$M_{ij}=M_{ij,0}+\Delta M_{ij}\qquad(6.6)$$

$$\left.\begin{aligned}&\vec{r}_G=\vec{r}_{G,0}+\Delta\vec{r}_G=(x_{G,0},y_{G,0},z_{G,0})^T+(\Delta x_G,\Delta y_G,\Delta z_G)\\&\vec{r}_B=\vec{r}_{B,0}+\vec{r}_B=(x_{B,0},0,z_{B,0})^T+(\Delta x_B,\Delta y_B,\Delta z_B)^T\end{aligned}\right\}\qquad(6.7)$$

$$\left.\begin{aligned}\Delta F_r&=(\bar{U}_{X,0}-\bar{W}_{X,0})(\Delta\bar{U}_X-\Delta\bar{W}_X)+(\bar{U}_{Z,0}-\bar{W}_{Z,0})(\Delta\bar{U}_Z-\Delta\bar{W}_Z)\\&=(\bar{U}_{X,0}-\bar{W}_{X,0})\Delta\bar{U}_X+(\bar{U}_{Z,0}-\bar{W}_{Z,0})\Delta\bar{U}_Z\\&\quad-\{(\bar{U}_{X,0}-\bar{W}_{X,0})\cos\theta_0+(\bar{U}_{Z,0}-\bar{W}_{Z,0})\sin\theta_0\}\cos\Psi\Delta\bar{W}_{X_E}\\&\quad-\{(\bar{U}_{X,0}-\bar{W}_{X,0})\cos\theta_0+(\bar{U}_{X,0}-\bar{W}_{Z,0})\sin\theta_0\}\sin\Psi\Delta\bar{W}_{Y_E}\\&\quad+\{(U_{X,0}-\bar{W}_{X,0})\sin\theta_0-(\bar{U}_{Z,0}-\bar{W}_{Z,0})\cos\theta_0\}\Delta\bar{W}_{Z_E}\\&\quad+(U_{X,0}W_{Z,0}-\bar{U}_{Z,0}\bar{W}_{X,0})\Delta\theta.\end{aligned}\right\}\qquad(6.8)$$

Combining equations (4.16), (4.17), (4.25) and (4.26) with the above perturbed relations the following linearized equations of motion can be obtained:

$$\left.\begin{aligned}&(X'_{U_X}\bar{D}+X_{U_X})\Delta\bar{U}_X+(X'_{U_Z}\bar{D}+X_{U_Z})\Delta\bar{U}_Z+(X''_\theta\bar{D}^2+X'_\theta\bar{D}+X_\theta)\Delta\theta\\&\quad+X_{U_Y}\Delta U_Y+(X_{\psi''}\bar{D}^2+X_\psi)\Delta\psi+X_\phi\Delta\phi\\&=(X'_{W,X_E}\bar{D}+X_{W,X_E})\Delta\bar{W}_{X_E}+(X'_{W,Y_E}\bar{D}+X_{W,Y_E})\Delta\bar{W}_{Y_E}\\&\quad+(X'_{W,Z_E}\bar{D}+X_{W,Z_E})\Delta\bar{W}_{Z_E}+X_M\Delta M+X_\delta\end{aligned}\right\}\text{ for surge}\qquad(6.9a)$$

$$\left.\begin{aligned}&(Z'_{U_X}\bar{D}+Z_{U_X})\Delta\bar{U}_X+(Z'_{U_Z}\bar{D}+Z_{U_Z})\Delta\bar{U}_Z+(Z''_\theta\bar{D}^2+Z'_\theta\bar{D}+Z_\theta)\Delta\theta\\&=(Z'_{W,X_E}D+Z_{W,X_E})\Delta\bar{W}_{X_E}+(Z'_{W,Y_E}D+Z_{W,Y_E})\Delta\bar{W}_{Y_E}\\&\quad+(Z_{\phi''}\bar{D}^2+Z'_\phi D)\Delta\phi+(z_{\phi''}\bar{D}^2)\Delta\psi+(Z'_{W,Z_E}\bar{D}+Z_{W,Z_E})\Delta\bar{W}_{Z_E}+Z_M\Delta M\end{aligned}\right\}\text{ for heave}\qquad(6.9b)$$

$$\left.\begin{aligned}&(M'_{U_X}\bar{D}+M_{U_X})\Delta\bar{U}_X+(M'_{U_Z}\bar{D}+M_{U_Z})\Delta\bar{U}_Z+(M_{\theta''}\bar{D}^2+M_{\theta'}\bar{D}+M_\theta)\Delta\theta\\&\quad+(M_{\phi'}\bar{D})\Delta\phi+(M_{\psi'}\bar{D})\Delta\psi\\&=(M_{W',X_E}\bar{D}+M_{W,X_E})\Delta\bar{W}_{X_E}+(M_{W',Y_E}\bar{D}+M_{W,Y_E})\Delta\bar{W}_{Y_E}\\&\quad+(M_{W',Z_E}\bar{D}+M_{W,Z_E})\Delta\bar{W}_{Z_E}\\&\quad+M_M\Delta\bar{M}+M_{x_G}\Delta\bar{x}_G+M_{x_B}\Delta\bar{x}_B+M_{z_G}\Delta\bar{z}_G+M_{z_B}\Delta\bar{z}_B\end{aligned}\right\}\text{for pitch}\quad(6.9c)$$

and

$$\left.\begin{aligned}&(Y_{U'_Y}\bar{D}+Y_{U_Y})\Delta\bar{U}_Y+(Y_{\phi''}\bar{D}^2+Y_{\phi'}\bar{D}+Y_\phi)\Delta\phi+(Y_{\psi''}\bar{D}^2+Y_{\psi'}\bar{D}+Y_\psi)\Delta\psi\\&\quad+Y_{U_X}\Delta\bar{U}_X+Y_{U_Z}\Delta\bar{U}_Z+(Y_{\theta'}\bar{D}+Y_\theta)\Delta\theta\\&=(Y_{W',Y_E}\bar{D}+Y_{W,X_E})\Delta\bar{W}_{X_E}+(Y_{W',Y_E}\bar{D}+Y_{W,Y_E})\Delta\bar{W}_{Y_E}+Y_{W,Z_E}\Delta\bar{W}_{Z_E}\end{aligned}\right\}\text{for sway}\quad(6.10a)$$

$$\left.\begin{aligned}&(L_{U'_Y}\bar{D}+L_{U_Y})\Delta\bar{U}_Y+(L_{\phi''}\bar{D}^2+L_{\phi'}\bar{D}+L_\phi)\Delta\phi+(L_{\psi''}\bar{D}^2+L_{\psi'}\bar{D}+L_\psi)\Delta\psi\\&\quad+L_{U_X}\Delta\bar{U}_X+(L_{U'_Z}\bar{D}+L_{U_Z})\Delta\bar{U}_Z+(L_{\theta'}\bar{D}+L_\theta)\Delta\theta\\&=(L_{W',X_E}\bar{D}+L_{W,X_E})\Delta\bar{W}_{X_E}+(L_{W',Y_E}\bar{D}+L_{W,Y_E})\Delta\bar{W}_{Y_E}\\&\quad+L_{W,Z_E}\Delta\bar{W}_{Z_E}+L_{y_G}\Delta\bar{y}_G+L_{y_B}\Delta\bar{y}_B\end{aligned}\right\}\text{for roll}\quad(6.10b)$$

$$\left.\begin{aligned}&(N_{U'_Y}\bar{D}+N_{U_Y})\Delta\bar{U}_Y+(N_{\phi''}\bar{D}^2+N_{\phi'}\bar{D}+N_\phi)\Delta\phi+(N_{\psi''}\bar{D}^2+N_{\psi'}\bar{D}+N_\psi)\Delta\psi\\&\quad+(N_{U'_X}\bar{D}+N_{U_X})\Delta\bar{U}_X+N_{U_Z}\Delta\bar{U}_Z+(N_{\theta'}\bar{D}+N_\theta)\Delta\theta\\&=(N_{W',X_E}\bar{D}+N_{W,X_E})\Delta\bar{W}_{X_E}+(N_{W',Y_E}\bar{D}+N_{W,Y_E})\Delta\bar{W}_{Y_E}\\&\quad+N_{W,Z_E}\Delta\bar{W}_{Z_E}+N_{y_G}\Delta\bar{y}_G+N_{y_B}\Delta\bar{y}_B+N_\delta\end{aligned}\right\}\text{for yaw}\quad(6.10c)$$

where

$$\bar{D}=d/d\bar{t},\qquad(6.11)$$

and

$$\left.\begin{aligned}X_{U_X}&=-(C_{F_X})_0|\bar{U}_{X,0}-\bar{W}_{X,0}|-2PC_{T_\lambda}/(\overline{R\Omega})\\X_{U_Y}&=-F_{r,0}(C_{F_X,\beta}/\bar{V}_0)\\X_{U'_Z}&=\bar{A}_{13}\\X_{U_Z}&=-(C_{F_X})_0|\bar{U}_{Z,0}-\bar{W}_{Z,0}|-F_{r,0}(C_{F_X,\alpha}/\bar{V}_0)\\X_{\theta''}&=\bar{M}_0\bar{z}_{G,0}+\bar{A}_{15}\\X_{\theta'}&=\bar{M}_0\bar{U}_{Z,0}+\bar{A}_{33}(\bar{U}_{Z,0}-\bar{W}_{Z,0})+\bar{A}_{13}(\bar{U}_{X,0}-2\bar{W}_{X,0})+\bar{A}_{11}\bar{W}_{Z,0}\\X_\theta&=-(1-\bar{M}_0)\cos\theta_0-(C_{F_X})_0(\bar{U}_{X,0}\bar{W}_{Z,0}-\bar{U}_{Z,0}\bar{W}_{X,0})\\&\quad+F_{r,0}(C_{F_X,\alpha}\bar{W}_{X,0}/\bar{V}_0)-2PC_{T_\lambda}\bar{W}_{Z,0}/(\overline{R\Omega})\\X_\phi&=F_{r,0}(C_{F_X,\beta}\bar{W}_{Z,0}/\bar{V}_0)\\X_{\psi''}&=-\bar{M}_0\bar{y}_{G,0}\cos\theta_0\\X_\psi&=-F_{r,0}C_{F_X,\beta}(\bar{W}_{X_E,0}\cos\Psi+\bar{W}_{Y_E,0}\sin\Psi)\end{aligned}\right\}\quad(6.12)$$

$$\left.\begin{aligned}
X_{W',X_E}&=\bar{A}_{11}\cos\Psi\cos\theta_0+\bar{A}_{13}\cos\Psi\sin\theta_0\\
X_{W,X_E}&=(C_{F_X})_0\{-(\bar{U}_{X,0}-\bar{W}_{X,0})\cos\theta_0-(\bar{U}_{Z,0}-\bar{W}_{Z,0})\sin\theta_0\}\cos\Psi\\
&\quad-F_{r,0}\{(C_{F_{X,\alpha}}/\bar{V}_0)\sin\theta_0\cos\Psi-(C_{F_{X,\beta}}/\bar{V}_0)\sin\Psi\}\\
&\quad-2PC_{T_\lambda}\cos\Psi\cos\theta_0/(\bar{R}\bar{\Omega})\\
X_{W',Y_E}&=\bar{A}_{11}\sin\Psi\cos\theta_0+\bar{A}_{13}\sin\Psi\sin\theta_0\\
X_{W,Y_E}&=-(C_{F_X})_0\{(\bar{U}_{X,0}-\bar{W}_{X,0})\cos\theta_0+(\bar{U}_{Z,0}-\bar{W}_{Z,0})\sin\theta_0\}\sin\Psi\\
&\quad-F_{r,0}\{(F_{F_{X,\alpha}}/\bar{V}_0)\sin\theta_0\sin\Psi+(C_{F_{X,\beta}}/\bar{V}_0)\cos\Psi\}\\
&\quad-2PC_{T_\lambda}\sin\Psi\cos\theta_0/(\bar{R}\bar{\Omega})\\
X_{W',Z_E}&=-\bar{A}_{11}\sin\theta_0+\bar{A}_{13}\cos\theta_0\\
X_{W,Z_E}&=-(C_{F_X})_0\{(\bar{U}_{Z,0}-\bar{W}_{Z,0})\cos\theta_0-(\bar{U}_{X,0}-\bar{W}_{X,0})\sin\theta_0\}\\
&\quad-F_{r,0}(C_{F_{X,\alpha}}/\bar{V}_0)\cos\theta_0+2PC_{T_\lambda}\sin\theta_0/(\bar{R}\bar{\Omega})\\
X_M&=-\sin\theta_0\\
X_\delta&=P\bar{F}_{TX}
\end{aligned}\right\}\qquad(6.13)$$

$$\left.\begin{aligned}
Z_{U_X'}&=\bar{A}_{13}\\
Z_{U_X}&=-(C_{F_Z})_0|U_{X,0}-W_{X,0}|\\
Z_{U_Z'}&=\bar{M}_0+\bar{A}_{33}-F_{r,0}(C_{F_{Z,\dot{\alpha}}}/\bar{V}_0)\\
Z_{U_Z}&=-(C_{F_Z})_0|\bar{U}_{Z,0}-\bar{W}_{Z,0}|-F_{r,0}(C_{F_{Z,\alpha}}+C_{F_{Z,\alpha^2}}|\alpha_0|)/\bar{V}_0)\\
Z_{\theta''}&=-\bar{M}_0\bar{x}_{G,0}+\bar{A}_{35}\\
Z_{\theta'}&=-\bar{M}_0\bar{U}_{X,0}-\bar{A}_{11}(\bar{U}_{X,0}-\bar{W}_{X,0})-\bar{A}_{33}\bar{W}_{X,0}-\bar{A}_{13}(\bar{U}_{Z,0}-2\bar{W}_{Z,0})\\
&\quad+F_{r,0}\{C_{F_{Z,\dot{\alpha}}}(\bar{W}_{X,0}/\bar{V}_0)-C_{F_{Z,q}}\}\\
Z_\theta&=-(1-\bar{M}_0)\sin\theta_0+(C_{F_Z})_0\{(\bar{U}_{Z,0}-\bar{W}_{Z,0})\bar{W}_{X,0}-(\bar{U}_{X,0}-\bar{W}_{X,0})\bar{W}_{Z,0}\}\\
&\quad+F_{r,0}(F_{F_{Z,\alpha}}+C_{F_{Z,\alpha^2}}|\alpha_0|)(\bar{W}_{X,0}/\bar{V}_0)\\
Z_{\phi''}&=\bar{M}_0\bar{y}_{G,0}\\
Z_{\phi'}&=-F_{r,0}C_{F_{Z,p}}\\
Z_{\psi''}&=-\bar{M}_0\bar{y}_{G,0}\sin\theta_0
\end{aligned}\right\}\qquad(6.14)$$

$$\left.\begin{aligned}
Z_{W',X_E}&=\{\bar{A}_{33}-F_{r,0}(C_{F_{Z,\dot{\alpha}}}/\bar{V}_0)\}\sin\theta_0\cos\Psi+\bar{A}_{13}\cos\Psi\cos\theta_0\\
Z_{W,X_E}&=(C_{F_Z})_0\{-(\bar{U}_{X,0}-\bar{W}_{X,0})\cos\theta_0-(\bar{U}_{Z,0}-\bar{W}_{Z,0})\sin\theta_0\}\cos\Psi\\
&\quad-F_{r,0}\{(C_{F_{Z,\alpha}}+C_{F_{Z,\alpha^2}}|\alpha_0|)/\bar{V}_0\}\sin\theta_0\cos\Psi\\
Z_{W',Y_E}&=(\bar{A}_{33}\sin\theta_0+\bar{A}_{13}\cos\theta_0)\sin\Psi-F_{r,0}(C_{F_{Z,\dot{\alpha}}}/\bar{V}_0)\sin\theta_0\sin\Psi\\
Z_{W,Y_E}&=-(C_{F_{Z,0}})\{(\bar{U}_{X,0}-\bar{W}_{X,0})\cos\theta_0+(\bar{U}_{Z,0}-\bar{W}_{Z,0})\sin\theta_0\}\sin\Psi\\
&\quad-F_{r,0}\{(C_{F_{Z,\alpha}}+C_{F_{Z,\alpha^2}}|\alpha_0|)/\bar{V}_0\}\sin\theta_0\sin\Psi\\
Z_{W',Z_E}&=\bar{A}_{33}\cos\theta_0-\bar{A}_{13}\sin\theta_0-F_{r,0}(C_{F_{Z,\dot{\alpha}}}/\bar{V}_0)\cos\theta_0\\
Z_{W,Z_E}&=-F_{r,0}\{(C_{F_{Z,\alpha}}+C_{F_{Z,\alpha^2}}|\alpha_0|)/\bar{V}_0\}\cos\theta_0-(C_{F_Z})_0\{(\bar{U}_{Z,0}-\bar{W}_{Z,0})\cos\theta_0\\
&\quad-(\bar{U}_{X,0}-\bar{W}_{X,0})\sin\theta_0\}\\
Z_M&=\cos\theta_0
\end{aligned}\right\}\qquad(6.15)$$

$$\left.\begin{aligned}
M_{U'_X}&=\bar{M}_0\bar{z}_{G,0}+\bar{A}_{15}\\
M_{U_X}&=-2\bar{A}_{13}(\bar{U}_{X,0}-\bar{W}_{X,0})+(\bar{A}_{11}-\bar{A}_{33})(\bar{U}_{Z,0}-\bar{W}_{Z,0})-(C_{M_Y})_0|\bar{U}_{X,0}-\bar{W}_{X,0}|\\
M_{U'_Z}&=-\bar{M}_0\bar{x}_{G,0}+\bar{A}_{35}-F_{r,0}(C_{M_Y,\dot{\alpha}}/\bar{V}_0)\\
M_{U_Z}&=2\bar{A}_{13}(\bar{U}_{Z,0}-\bar{W}_{Z,0})+(\bar{A}_{11}-\bar{A}_{33})(\bar{U}_{X,0}-\bar{W}_{X,0})\\
&\quad -F_{r,0}(C_{M_Y,\alpha}/\bar{V}_0)-(C_{M_Y})_0|\bar{U}_{Z,0}-\bar{W}_{Z,0}|\\
M_{\theta''}&=\bar{I}_{Y,0}+\bar{A}_{55}\\
M_{\theta'}&=(\bar{M}_0\bar{z}_{G,0}+\bar{A}_{15})\bar{U}_{Z,0}+(\bar{M}\bar{x}_{G,0}-\bar{A}_{35})\bar{U}_{X,0}\\
&\quad +F_{r,0}\{-C_{M_Y,q}+C_{M_Y,\dot{\alpha}}(\bar{W}_{X,0}/\bar{V}_0)\}\\
M_{\theta}&=(\bar{M}_0\bar{z}_{G,0}-\bar{z}_{B,0})\cos\theta_0-(\bar{M}_0\bar{x}_{G,0}-\bar{x}_{B,0})\sin\theta_0-\{2\bar{A}_{13}(\bar{U}_{Z,0}-\bar{W}_{Z,0})\\
&\quad +(\bar{A}_{11}-\bar{A}_{33})(\bar{U}_{X,0}-\bar{W}_{X,0})\}\bar{W}_{X,0}+\{-2\bar{A}_{13}(\bar{U}_{X,0}-\bar{W}_{X,0})\\
&\quad +(\bar{A}_{11}-\bar{A}_{33})(\bar{U}_{Z,0}-\bar{W}_{Z,0})\}\bar{W}_{Z,0}+F_{r,0}C_{M_Y,\alpha}(\bar{W}_{X,0}/\bar{V}_0)\\
&\quad -(C_{M_Y})_0\{(\bar{U}_{X,0}-\bar{W}_{X,0})\bar{W}_{Z,0}-(\bar{U}_{Z,0}-\bar{W}_{Z,0})\bar{W}_{X,0}\}\\
M_{\phi'}&=-F_{r,0}C_{M_Y,p}\\
M_{\psi'}&=-F_{r,0}C_{M_Y,r}
\end{aligned}\right\}\quad(6.16)$$

$$\left.\begin{aligned}
M_{W'X_E}&=(\bar{A}_{15}\cos\theta_0+\bar{A}_{35}\sin\theta_0)\cos\Psi-F_{r,0}(C_{M_Y,\dot{\alpha}}/\bar{V}_0)\sin\theta_0\cos\Psi\\
M_{W,X_E}&=[2A_{13}\{(\bar{U}_{Z,0}-\bar{W}_{Z,0})\sin\theta_0-(\bar{U}_{X,0}-\bar{W}_{X,0})\cos\theta_0\}\\
&\quad +(\bar{A}_{11}-\bar{A}_{33})\{(\bar{U}_{X,0}-\bar{W}_{X,0})\sin\theta_0+(\bar{U}_{Z,0}-\bar{W}_{Z,0})\cos\theta_0\}]\cos\Psi\\
&\quad +(C_{M_Y})_0\{-(\bar{U}_{X,0}-\bar{W}_{X,0})\cos\theta_0+(\bar{U}_{Z,0}-\bar{W}_{Z,0})\sin\theta_0\}\cos\Psi\\
&\quad -\bar{F}_{r,0}(C_{M_Y,\alpha}/\bar{V}_0)\sin\theta_0\cos\Psi\\
M_{W',Y_E}&=(\bar{A}_{15}\cos\theta_0+\bar{A}_{35}\sin\theta_0)\sin\Psi-F_{r,0}(C_{M_Y,\dot{\alpha}}/\bar{V}_0)\sin\theta_0\sin\Psi\\
M_{W,Y_E}&=[2\bar{A}_{13}\{(\bar{U}_{Z,0}-\bar{W}_{Z0})\sin\theta_0-(\bar{U}_{X,0}-\bar{W}_{X,0})\cos\theta_0\}\\
&\quad +(\bar{A}_{11}-\bar{A}_{33})\{(\bar{U}_{X,0}-\bar{W}_{X,0})\sin\theta_0+(\bar{U}_{Z,0}-\bar{W}_{Z,0})\cos\theta_0\}]\sin\Psi\\
&\quad -(C_{M_Y})_0\{(\bar{U}_{X,0}-\bar{W}_{X,0})\cos\theta_0+(\bar{U}_{Z,0}-\bar{W}_{Z,0})\sin\theta_0\}\sin\Psi\\
&\quad -F_{r,0}(C_{M_Y,\alpha}/\bar{V}_0)\sin\theta_0\sin\Psi\\
M_{W',Z_E}&=-\bar{A}_{15}\sin\theta_0+\bar{A}_{35}\cos\theta_0-F_{r,0}(C_{M_Y,\dot{\alpha}}/\bar{V}_0)\cos\theta_0\\
M_{W,Z_E}&=2\bar{A}_{13}\{(\bar{U}_{Z,0}-\bar{W}_{Z,0})\cos\theta_0+(\bar{U}_{X,0}-\bar{W}_{X,0})\sin\theta_0\}\\
&\quad +(\bar{A}_{11}-\bar{A}_{33})\{\bar{U}_{X,0}-\bar{W}_{X,0})\cos\theta_0+(\bar{U}_{Z,0}-\bar{W}_{Z,0})\sin\theta_0\}\\
&\quad -(C_{M_Y})_0\{(\bar{U}_{Z,0}-\bar{W}_{Z,0})\cos\theta_0-(\bar{U}_{X,0}-\bar{W}_{X,0})\sin\theta_0\}\\
&\quad -F_{r,0}(C_{M_Y,\alpha}/\bar{V}_0)\cos\theta_0\\
M_M&=-\bar{x}_{G,0}\cos\theta_0-\bar{z}_{G,0}\sin\theta_0\\
M_{x_G}&=-\bar{M}_0\cos\theta_0\\
M_{X_B}&=\cos\theta_0\\
M_{z_G}&=-\bar{M}_0\sin\theta_0\\
M_{z_B}&=\sin\theta_0
\end{aligned}\right\}\quad(6.17)$$

$$
\left.\begin{aligned}
Y_{U'_Y} &= \bar{M}_0 + \bar{A}_{22} - F_{r,0}(C_{F_Y,\dot{\beta}}/\bar{V}_0) \\
Y_{U_Y} &= -F_{r,0}(C_{F_Y,\beta}/\bar{V}_0) \\
Y_{U_X} &= -(C_{F_Y,0})\,|\bar{U}_{X,0} - \bar{W}_{X,0}| \\
Y_{U_Z} &= -(C_{F_Y,0})\,|\bar{U}_{Z,0} - \bar{W}_{Z,0}| \\
Y_{\phi''} &= \bar{M}_0\bar{z}_{G,0} + \bar{A}_{24} \\
Y_{\phi'} &= -M_0\bar{U}_{Z,0} - \bar{A}_{33}(\bar{U}_{Z,0} - \bar{W}_{Z,0}) - \bar{A}_{22}\bar{W}_{Z,0} - \bar{A}_{13}(\bar{U}_{X,0} - \bar{W}_{X,0}) \\
&\quad + F_{r,0}\{-C_{F_Y,p} + C_{F_Y,\dot{\beta}}(\bar{W}_{Z,0}/\bar{V}_0)\} \\
Y_{\phi} &= (1 - \bar{M}_0)\cos\theta_0 + F_{r,0}(C_{Y_\beta}/\bar{V}_0)\bar{W}_{Z0} \\
Y_{\psi''} &= (\bar{M}_0\bar{x}_{G,0} + \bar{A}_{26})\cos\theta_0 + (\bar{M}_0\bar{z}_{G,0} - \bar{A}_{24})\sin\theta_0 \\
Y_{\psi'} &= (\bar{M}_0 + \bar{A}_{11})\bar{U}_{X,0} - \bar{A}_{11}\bar{W}_{X,0} + \bar{A}_{13}(\bar{U}_{Z,0} - \bar{W}_{Z,0})\}\cos\theta_0 \\
&\quad + \{(\bar{M}_0 + \bar{A}_{33})\bar{U}_{Z,0} - \bar{A}_{33}\bar{W}_{Z,0} + \bar{A}_{13}(\bar{U}_{X,0} - \bar{W}_{X,0})\}\sin\theta_0 \\
&\quad + \bar{A}_{22}(\bar{W}_{X_E,0}\cos\Psi + W_{Y_E,0}\sin\Psi) - F_{r,0}\{C_{F_Y,r} \\
&\quad + C_{F_Y,\dot{\beta}}(\bar{W}_{X_E,0}\cos\Psi + \bar{W}_{Y_E,0}\sin\Psi)\} \\
Y_{\psi} &= -F_{r,0}C_{F_Y,\beta}(\bar{W}_{X_E,0}\cos\Psi + \bar{W}_{Y_E,0}\sin\Psi)/\bar{V}_0 \\
Y_{\theta'} &= -F_{r,0}C_{F_Y,q} \\
Y_{\theta} &= -(C_{F_Y})_0\{(\bar{U}_{X,0} - \bar{W}_{X,0})\bar{W}_{Z,0} - (\bar{U}_{Z,0} - \bar{W}_{Z,0})\bar{W}_{X,0}\}
\end{aligned}\right\} \quad (6.18)
$$

$$
\left.\begin{aligned}
Y_{W',X_E} &= \{-A_{22} + F_{r,0}(C_{F_Y,\dot{\beta}}/\bar{V}_0)\}\sin\Psi \\
Y_{W,X_E} &= -(C_{F_Y})_0\{(\bar{U}_{X,0} - \bar{W}_{X,0})\cos\theta_0 + (\bar{U}_{Z,0} - \bar{W}_{Z,0})\sin\theta_0\}\cos\Psi \\
&\quad + F_{r,0}(C_{F_Y,\beta}/\bar{V}_0)\sin\Psi \\
Y_{W',Y_E} &= \{\bar{A}_{22} - F_{r,0}(C_{F_Y,\dot{\beta}}/\bar{V}_0)\}\cos\Psi \\
Y_{W,Y_E} &= -(C_{F_Y})_0\{(\bar{U}_{X,0} - \bar{W}_{X,0})\cos\theta_0 + (\bar{U}_{Z,0} - \bar{W}_{Z,0})\sin\theta_0\}\sin\Psi \\
&\quad - F_{r,0}(C_{F_Y,\beta}/\bar{V}_0)\cos\Psi \\
Y_{W,Z_E} &= (C_{F_Y})_0\{(\bar{U}_{X,0} - \bar{W}_{X,0})\sin\theta_0 - (\bar{U}_{Z,0} - \bar{W}_{Z,0})\cos\theta_0\}
\end{aligned}\right\} \quad (6.19)
$$

$$
\left.\begin{aligned}
L_{U'_Y} &= -\bar{M}_0\bar{z}_{G,0} + \bar{A}_{24} - F_{r,0}(C_{M_X,\dot{\beta}}/\bar{V}_0) \\
L_{U_Y} &= \bar{A}_{13}(\bar{U}_{X,0} - \bar{W}_{X,0}) - (A_{22} - \bar{A}_{33})(U_{Z,0} - \bar{W}_{Z,0}) - F_{r,0}(C_{M_X,\beta}/\bar{V}_0) \\
L_{U_X} &= -(C_{M_X})_0\,|U_{X,0} - W_{X,0}| \\
L_{U'_Z} &= \bar{M}_0\bar{y}_{G,0} \\
L_{U_Z} &= -(C_{M_X})_0\,|\bar{U}_{Z,0} - \bar{W}_{Z,0}| \\
L_{\phi''} &= \bar{I}_{X,0} + \bar{A}_{44} \\
L_{\phi'} &= (M_0\bar{z}_{G,0} - A_{24})\bar{U}_{Z,0} - F_{r,0}(C_{M_X\,p} - C_{M_X,\dot{\beta}}(\bar{W}_{Z,0}/\bar{V}_0)\} \\
L_{\phi} &= (\bar{M}_0\bar{z}_{G,0} - \bar{z}_{B,0})\cos\theta_0 - \{\bar{A}_{13}(\bar{U}_{X,0} - \bar{W}_{X,0}) \\
&\quad - (\bar{A}_{22} - \bar{A}_{33})(U_{Z,0} - \bar{W}_{Z,0})\}\bar{W}_{Z,0} + F_{r,0}C_{M_X,\beta}(\bar{W}_{Z,0}/\bar{V}_0) \\
L_{\psi''} &= (-\bar{J}_{XZ,0} + \bar{A}_{46})\cos\theta_0 - (\bar{I}_{X,0} + \bar{A}_{44})\sin\theta_0 \\
L_{\psi'} &= \{-(\bar{M}_0\bar{z}_{G,0} + \bar{A}_{15})\bar{U}_{X,0} + A_{14}\bar{W}_{X,0} - (\bar{A}_{26} + \bar{A}_{35})(\bar{U}_{Z,0} - \bar{W}_{Z,0})\}\cos\theta_0 \\
&\quad - \{(\bar{M}_0\bar{z}_{G,0} - \bar{A}_{24})\bar{U}_{Z,0} + A_{24}\bar{W}_{Z,0}\}\sin\theta_0 + \bar{A}_{24}(\bar{W}_{X_E,0}\cos\Psi \\
&\quad + \bar{W}_{Y_E,0}\sin\Psi) - F_{r,0}\{C_{M_X,r} + C_{M_X,\dot{\beta}}(\bar{W}_{X_E,0}\cos\Psi + W_{Y_E,0}\sin\Psi)/\bar{V}_0\}
\end{aligned}\right\} \quad (6.20)
$$

$$\left.\begin{aligned}
L_{\psi}&=\{\bar{A}_{13}(\bar{U}_{X,0}-\bar{W}_{X,0})-(\bar{A}_{22}-\bar{A}_{33})(\bar{U}_{Z,0}-\bar{W}_{Z,0})\}(\bar{W}_{X_E,0}\cos\Psi\\
&\quad+\bar{W}_{Y_E,0}\sin\Psi)-F_{r,0}C_{M_X,\beta}(\bar{W}_{X_E,0}\cos\Psi+\bar{W}_{Y_E,0}\sin\Psi)/\bar{V}_0\\
L_{\theta'}&=-\bar{M}_0\bar{y}_{G,0}\bar{U}_{X,0}-F_{r,0}C_{M_X,q}\\
L_{\theta}&=\bar{M}_0\bar{y}_{G,0}\sin\theta_0-(C_{M_X})_0\{(\bar{U}_{X,0}-\bar{W}_{X,0})\bar{W}_{Z,0}-(\bar{U}_{Z,0}-\bar{W}_{Z,0})\bar{W}_{X,0}\}
\end{aligned}\right\}$$

$$\left.\begin{aligned}
L_{W',X_E}&=\{-\bar{A}_{24}+F_{r,0}(C_{M_X,\dot{\beta}}/\bar{V}_0)\}\sin\Psi\\
L_{W,X_E}&=-\{\bar{A}_{13}(\bar{U}_{X,0}-\bar{W}_{X,0})-(\bar{A}_{22}-\bar{A}_{33})(\bar{U}_{Z,0}-\bar{W}_{Z,0})\}\sin\Psi\\
&\quad-(C_{M_X})_0\{(\bar{U}_{X,0}-\bar{W}_{X,0})\cos\theta_0+(\bar{U}_{Z,0}-\bar{W}_{Z,0})\sin\theta_0\}\cos\Psi\\
&\quad+F_{r,0}(C_{M_X,\beta}/\bar{V}_0)\sin\Psi\\
L_{W',Y_E}&=\{\bar{A}_{24}-F_{r,0}(C_{M_X,\dot{\beta}}/\bar{V}_0)\}\cos\Psi\\
L_{W,Y_E}&=\{\bar{A}_{13}(\bar{U}_{X,0}-\bar{W}_{X,0})-(\bar{A}_{22}-\bar{A}_{33})(\bar{U}_{Z,0}-\bar{W}_{Z,0})\}\cos\Psi\\
&\quad-(C_{M_X})_0\{(\bar{U}_{X,0}-\bar{W}_{X,0})\cos\theta_0+(\bar{U}_{Z,0}-\bar{W}_{Z,0})\sin\theta_0\}\sin\Psi\\
&\quad-F_{r,0}(C_{M_X,\beta}/\bar{V}_0)\cos\Psi\\
L_{W,Z_E}&=-(C_{M_X})_0\{(\bar{U}_{Z,0}-\bar{W}_{Z,0})\cos\theta_0-(\bar{U}_{X,0}-\bar{W}_{X,0})\sin\theta_0\}\\
L_{y_G}&=\bar{M}_0\cos\theta_0\\
L_{y_B}&=-\cos\theta_0
\end{aligned}\right\}\quad(6.21)$$

$$\left.\begin{aligned}
N_{U'_Y}&=\bar{M}_0\bar{x}_{G,0}+\bar{A}_{26}-F_{r,0}(C_{M_Z,\dot{\beta}}/\bar{V}_0)\\
N_{U_Y}&=-\{\bar{A}_{13}(\bar{U}_{Z,0}-\bar{W}_{Z,0})+(\bar{A}_{11}-\bar{A}_{22})(\bar{U}_{X,0}-\bar{W}_{X,0})\}-F_{r,0}(C_{M_X,\beta}/\bar{V}_0)\\
N_{U'_X}&=-\bar{M}_0\bar{y}_{G,0}\\
N_{U_X}&=-(C_{M_Z})_0|\bar{U}_{X,0}-\bar{W}_{X,0}|\\
N_{U_Z}&=-(C_{M_Z})_0|\bar{U}_{Z,0}-\bar{W}_{Z,0}|\\
N_{\phi''}&=-\bar{J}_{XZ,0}+\bar{A}_{46}\\
N_{\phi'}&=-\bar{M}_0\bar{x}_{G,0}\bar{W}_{Z,0}+\bar{A}_{35}(\bar{U}_{Z,0}-\bar{W}_{Z,0})-\bar{A}_{26}\bar{W}_{Z,0}+(\bar{A}_{16}+\bar{A}_{24})\bar{U}_{X,0}-\bar{W}_{X,0})\\
&\quad-\bar{F}_{r,0}\{C_{M_Z,p}-C_{M_Z,\dot{\beta}}(\bar{W}_{Z,0}/\bar{V}_0)\}\\
N_{\phi}&=-(\bar{M}_0\bar{x}_{G,0}-\bar{x}_{B,0})\cos\theta_0+\{\bar{A}_{13}(\bar{U}_{X,0}-\bar{W}_{X,0})\\
&\quad+(\bar{A}_{11}-\bar{A}_{22})(\bar{U}_{X,0}-\bar{W}_{X,0})\}\bar{W}_{Z,0}+F_{r,0}C_{M_Z,\beta}(\bar{W}_{Z,0}/\bar{V}_0)\\
N_{\psi''}&=(\bar{I}_{Z,0}+\bar{A}_{66})\cos\theta_0+(\bar{J}_{XZ,0}-\bar{A}_{46})\sin\theta_0\\
N_{\psi'}&=\{\bar{M}_0\bar{x}_{G,0}+A_{26})\bar{U}_{Z,0}-A_{26}W_{X,0}\}\cos\theta_0+\{(\bar{M}_0\bar{x}_{G,0}-\bar{A}_{35})\bar{U}_{Z,0}+\bar{A}_{35}W_{X,0}\\
&\quad-(\bar{A}_{15}+\bar{A}_{24})(\bar{U}_{X,0}-\bar{W}_{X,0})\}\sin\theta_0+\bar{A}_{26}(\bar{W}_{X_E,0}\cos\Psi+\bar{W}_{Y_E}\sin\Psi)\\
&\quad-F_{r,0}\{C_{M_Z,r}+C_{M_Z,\dot{\beta}}(\bar{W}_{X_E,0}\cos\Psi+\bar{W}_{Y_E,0}\sin\Psi)/\bar{V}_0\}\\
&\quad-P(b/2V_B^{1/3})C_{T_\lambda}/(\overline{R\Omega})\\
N_{\psi}&=-\{A_{13}(\bar{U}_{Z,0}-\bar{W}_{Z,0})+(\bar{A}_{11}-\bar{A}_{22})(\bar{U}_{X,0}-\bar{W}_{X,0})\}(\bar{W}_{X_E,0}\cos\Psi\\
&\quad+\bar{W}_{Y_E,0}\sin\Psi)-F_{r,0}C_{M_Z,\beta}(\bar{W}_{X_E,0}\cos\Psi+\bar{W}_{Y_E,0}\sin\Psi)\\
N_{\theta'}&=-M_0\bar{y}_{G,0}\bar{U}_{Z,0}-F_{r,0}(C_{M_Z,q})\\
N_{\theta}&=-\bar{M}_0\bar{y}_{G,0}\cos\theta_0-(C_{M_Z})_0\{(\bar{U}_{X,0}-\bar{W}_{X,0})\bar{W}_{Z,0}-(\bar{U}_{Z,0}-\bar{W}_{Z,0})\bar{W}_{X,0}\}
\end{aligned}\right\}\quad(6.22)$$

$$\left.\begin{aligned}
N_{W',X_E}&=-\bar{A}_{26}\sin\Psi+F_{r,0}(C_{M_Z,\dot\beta}/\bar{V}_0)\sin\Psi\\
N_{W,X_E}&=\{\bar{A}_{13}(\bar{U}_{Z,0}-\bar{W}_{Z,0})+(\bar{A}_{11}-\bar{A}_{22})(\bar{U}_{X,0}-\bar{W}_{X,0})\}\sin\Psi\\
&\quad-(C_{M_Z})_0\{(\bar{U}_{X,0}-\bar{W}_{X,0})\cos\theta_0+(\bar{U}_{Z,0}-\bar{W}_{Z,0})\sin\theta_0\}\cos\Psi\\
&\quad+F_{r,0}(C_{M_Z,\beta}/\bar{V}_0)\sin\Psi\\
N_{W',Y_E}&=\bar{A}_{26}\cos\Psi-F_{r,0}(C_{M_Z,\dot\beta}/\bar{V}_0)\cos\Psi\\
N_{W,Y_E}&=-\{\bar{A}_{13}(\bar{U}_{Z,0}-\bar{W}_{Z,0})+(\bar{A}_{11}-\bar{A}_{22})(\bar{U}_{X,0}-\bar{W}_{X,0})\}\cos\Psi\\
&\quad-(C_{M_Z})_0\{(\bar{U}_{X,0}-\bar{W}_{X,0})\cos\theta_0+(\bar{U}_{Z,0}-\bar{W}_{Z,0})\sin\theta_0\}\sin\Psi\\
&\quad-F_{r,0}(C_{M_Z,\beta}/\bar{V}_0)\cos\Psi\\
N_{W,Z_E}&=-(C_{M_Z})_0\{(\bar{U}_{Z,0}-\bar{W}_{Z,0})\cos\theta_0-(\bar{U}_{X,0}-\bar{W}_{X,0})\sin\theta_0\}\\
N_\delta&=P\bar{M}_{T_Z}\\
N_{y_G}&=\bar{M}_0\sin\theta_0\\
N_{y_B}&=-\sin\theta_0.
\end{aligned}\right\}\qquad(6.23)$$

TABLE 8 Derivatives or coefficient of equations of motion

Items	Number	Items	Number
$X_{U'_X}$	1.160	$N_{U'_Y}$	-0.546
X_{U_X}	$0.130\bar{V}_{X,0}$	N_{U_Y}	$-0.2(\bar{U}_{X,0}-\bar{W}_{X,0})$
$Y_{U'_Y}$	2.121	$N_{\psi''}$	1.184
Y_{U_Y}	$0.9\bar{V}_0$	$N_{\psi'}$	$1.59W_{X,0}$
$Y_{\psi'}$	$1.088\bar{U}_{X,0}-1.011\bar{W}_{X,0}$ $-\bar{V}_0{}^2\bar{W}_{X,0}$	N_ψ	$-0.2W^2{}_{X,0}$
Y_ψ	$-0.\bar{V}\bar{W}_{X,0}$		

Some of necessary derivatives used in the perturbed motion from a steady straight flight are listed in Table 8.

(i) Response of Forward Speed

The flight speed is controlled by the change of thrust. Equation (6.9a) for surging motion may be simplified as

$$(X_{U'_X}\bar{D}+X_{U_X})\Delta\bar{U}_X=X_\delta. \qquad (6.24)$$

Then the solution for a step input of X_δ can be given by

$$\Delta\bar{U}_X(\bar{t})=(X_\delta/X_{U_X})\{1-\exp(-\bar{t}/\bar{T}_X)\} \qquad (6.25)$$

where

$$\bar{T}_X=X_{U'_X}/X_{U_X}. \qquad (6.26)$$

Fig. 9 shows the above result compared with a test result of the vehicle, which has been obtained from a flight recorder installed on the vehicle in operation in

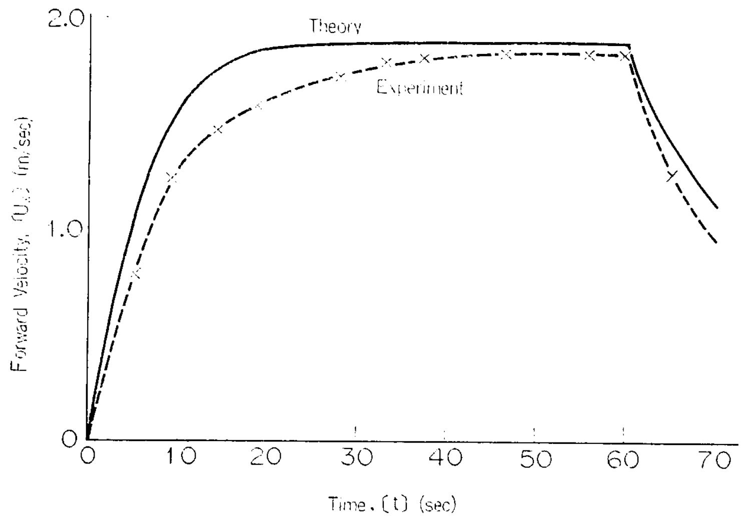

FIG. 9. Time response of surging motion for a step input of thrust

the sea. The discrepancy between theory and experiment must be resulted from the inadequate drag estimation due to neglect the change of Reynolds number during the flight.

(ii) Vertical Ascent or Descent

The ascending or descending speed can effectively be controlled by the change of mass or change of difference between buoyant and gravity forces for low speed flight and by the change of attitude angle of the vehicle in high forward speed. Here, let us consider the former case. Equation (6.9b) for heaving motion may be approximately rewritten as

$$(Z_{U'_Z}\bar{D}+Z_{U_Z})\Delta\bar{U}_Z=\Delta\bar{M}, \tag{6.27}$$

and its solution for a step input of $-\Delta\bar{M}$ for ascending and $+\Delta M$ for decending motion can be given by

$$\Delta\bar{U}_Z(\bar{t})=\mp(1/Z_{U_Z})(1-e^{-t/T_Z})\Delta\bar{M} \tag{6.28}$$

where

$$\bar{T}_Z=Z_{U'_Z}/Z_{U_Z}\cong\{(\bar{M}+\bar{A}_{33})_0+F_{r,0}(C_{F_{Z,\alpha'}}/\bar{V}_0)\}/\{-(C_{F_Z})_0|\bar{U}_{Z,0}-\bar{W}_{Z,0}|\} \tag{6.29}$$

The time history of the vertical velocity for a step input of ballast change or weight drop is completely similar to Fig. 9. It is interesting to note that the additional mass, A_{33}, is usually larger than the mass, M, when the vehicle is prepared with tail surfaces for the stability.

(iii) Response of Attitude Change

By moving the ballast in the longitudinal direction the attitude change in vertical plane will be resulted. Then the equation of pure pitching motion and its solution can respectively be given by

$$(M_{\theta''}\bar{D}^2+M_{\theta'}\bar{D}+M_\theta)\Delta\theta=-\bar{M}_0\Delta\bar{x}_G \tag{6.30}$$

$$\Delta\theta(\bar{t}) = -(\overline{M}_0/M_\theta)\Delta\bar{x}_G[1+\{S_2/(S_1-S_2)\}e^{S_1 t}+\{S_1/(S_2-S_1)\}e^{S_2 t}] \tag{6.31}$$

where

$$S_{\frac{1}{2}} = (1/2)\{-(M_{\theta'}/M_{\theta''}) \pm \sqrt{(M_{\theta'}/M_{\theta''})^2 - 4(M_\theta/M_{\theta''})}\} \tag{6.32}$$

and where $M_{\theta''}$ is always positive.

As well known, if either $M_{\theta'}$ is positive or M_θ is negative o rzero the system has divergent characteristics; if $M_{\theta'}$ is zero and M_θ is positive the system is a neutrally oscillatory motion; and if $M_{\theta'}$ is negative and M_θ is positive the system is stable and has an oscillatory convergent motion for $(M_{\theta'}/M_{\theta''})^2 < 4(M_\theta/M_{\theta''})$ or a nonoscillatory motion comprised of two monotonically comvergent motions for $(M_{\theta'}/M_{\theta''}) \geq 4(M_\theta/M_{\theta''})$.

In either stable motion the damping is solely obtained from the hydrodynamic damping, whereas the restoring moment can be given by both the hydrodynamic and hydrostatic or buoyant moments.

(iv) Motion in Vertical Plane

By neglecting the cross couppled terms with lateral motion a complete set of longitudinal equations, equations (6.9), specifies the dynamic behaviour of the vehicle in the vertical plane. The characteristic equations of these linearized equations,

$$\left.\begin{aligned}
D(S) = {} & S^4\{X_{U'_X}Z_{U'_Z}M_{\theta''} - X_{\theta''}Z_{U'_Z}M_{U'_X} - X_{U'_X}Z_{\theta''}M_{U'_Z}\} \\
& + S^3\{X_{U_X}Z_{U'_Z}M_{\theta''} + X_{U'_X}Z_{U_X}M_{\theta''} + X_{U'_X}Z_{U'_Z}M_{\theta'} + X_{U_Z}Z_{\theta''}M_{U'_X} \\
& + X_{\theta''}Z_{U_X}M_{U'_Z} - X_{\theta''}Z_{U'_Z}M_{U_X} - X_{\theta''}Z_{U_Z}M_{U'_X} - X_{\theta'}Z_{U'_Z}M_{U'_X} \\
& - X_{U'_X}Z_{\theta''}M_{U_Z} - X_{U_X}Z_{\theta''}M_{U'_Z} - X_{U_X}Z_{\theta''}M_{U'_Z}\} \\
& + S^2\{X_{U_X}Z_{U_Z}M_{\theta''} + X_{U'_X}Z_{U'_Z}M_\theta + X_{U'_X}Z_{U_Z}M_{\theta'} + X_{U_X}Z_{U'_Z} + M_{\theta'} \\
& + X_{U_Z}Z_{\theta''}M_{U_X} + X_{U_Z}Z_{\theta'}M_{U'_X} + X_{\theta''}Z_{U_X}M_{U_Z} + X_{\theta'}Z_{U_X}M_{U'_Z} \\
& - X_{\theta''}Z_{U_Z}M_{U_X} - X_{\theta'}Z_{U'_Z}M_{U_X} - X_{\theta'}Z_{U_Z}M_{U'_X} - X_\theta Z_{U'_Z}M_{U'_X} \\
& - X_{U'_X}Z_{\theta'}M_{U_Z} - X_{U'_X}Z_\theta M_{U'_X} - X_{U_X}Z_{\theta'}M_{U'_Z} - X_{U_Z}Z_{U_X}M_{\theta''} \\
& + S\{X_{U'_X}Z_{U_Z}M_\theta + X_{U_X}Z_{U'_Z}M_\theta + X_{U_X}Z_{U_Z}M_{\theta'} + X_{U_Z}Z_{\theta'}M_{U_X} \\
& + X_{U_Z}Z_\theta M_{U'_X} + X_{\theta'}Z_{U_X}M_{U_Z} + X_\theta Z_{U_X}M_{U'_Z} \\
& - X_{\theta'}Z_{U_Z}M_{U_X} - X_\theta Z_{U'_Z}M_{U_X} - X_\theta Z_{U_Z}M_{U'_X} - X_{U'_X}Z_\theta M_U \\
& - X_{U_X}Z_{\theta'}M_{U_Z} - X_{U_X}Z_\theta M_{U'_Z} - X_{U_Z}Z_{U_X}M_{\theta'}\} \\
& + \{X_{U_X}Z_{U_Z}M_\theta + X_{U_Z}Z_\theta M_{U_X} + X_\theta Z_{U_X}M_{U_Z} \\
& - X_\theta Z_{U_Z}M_{U_X} - X_{U_X}Z_\theta M_{U_Z} - X_{U_Z}Z_{U_X}M_\theta\} = 0
\end{aligned}\right\} \tag{6.33}$$

have usually two real roots and a pair of complex roots, all of which are close to those given by the preceding simplified equations. Since there are no positive lifting surface for the present submersible socalled phugoyed oscillation being familiar in the airplane dynamics has not been observed.

(v) Rolling Motion

The rolling motion in the immersed vehicles is mainly governed by the vertical distance between the center of gravity and the center of buoyancy. Different from surface vessels the center of buoyancy is over the center of gravity so that the vehicle is inherently stabilized for the rolling motion in any rolling angle. This arrangement is earnestly necessary because there is no hydrodynamic restoring moment at any flight speed in wingless vehicles.

The equation of pure rolling motion can be derived from equation (6.10b) as follows:

$$(L_{\phi''}\bar{D}^2+L_{\phi'}\bar{D}+L_{\phi})\Delta\phi=(\bar{M}_0\cos\theta_0)\Delta\bar{y}_G. \tag{6.34}$$

The above equation has a solution of a lightly damped sinusoidal oscillation in usual immersed vehicle such as

$$\left.\begin{aligned}\Delta\phi(\bar{t})=(\bar{M}_0/L_{\phi})\Delta\bar{y}_G[1-e^{-\zeta\omega_n\bar{t}}\{\sqrt{1-\zeta^2}\cos(\omega_n\sqrt{1-\zeta^2}\bar{t})\\ +\zeta\sin(\omega_n\sqrt{1-\zeta^2}\bar{t})\}/\sqrt{1-\zeta^2}]\end{aligned}\right\} \tag{6.35}$$

where

$$\left.\begin{aligned}\omega_n&=\sqrt{L_{\phi}/L_{\phi''}}=\sqrt{\bar{M}_0(\bar{z}_G-\bar{z}_B)_0/(\bar{I}_X+\bar{A}_{44})_0}\\ 2\zeta\omega_n&=L_{\phi'}/L_{\phi''}=-F_{r,0}C_{M_X,\phi'}/(\bar{I}_X+\bar{A}_{44})_0).\end{aligned}\right\} \tag{6.36}$$

It must be careful to have too large positive metacentric height, $\bar{z}_G-\bar{z}_B$, so as to have too rapid rolling motion with poor damping.

(vi) Lateral Motion

A typical lateral motion in horizontal plane is a coupling motion of yawing angular motion and lateral translation under a constant speed without any current. This can be, from equation (6.10), approximated by

$$\left.\begin{aligned}(Y_{U'_Y}\bar{D}+Y_{U_Y})\Delta\bar{U}_Y+(Y_{\psi''}\bar{D}^2+Y_{\psi'}\bar{D})\Delta\psi=0\\ (N_{U_Y'}\bar{D}+N_{U_Y})\Delta\bar{U}_Y+(N_{\psi''}\bar{D}^2+N_{\psi'}\bar{D})\Delta\psi=N_{\delta},\end{aligned}\right\} \tag{6.37}$$

the characteristic equation of which is given by

$$D(S)=(Y_{U_Y'}N_{\psi''}-Y_{\psi''}N_{U'_Y})S(S^2+2\zeta\omega_nS+\omega_N^2)=0 \tag{6.38}$$

where

$$\left.\begin{aligned}2\zeta\omega_n&=(Y_{U'_Y}N_{\psi'}+Y_{U_Y}N_{\psi''}-Y_{\psi'}N_{U'_Y}-Y_{\psi''}N_{U_Y})/(Y_{U'_Y}N_{\psi''}-Y_{\psi''}N_{U'_Y})\\ \omega_n^2&=(Y_{U_Y}N_{\psi'}-Y_{\psi'}N_{U_Y})/(Y_{U'_Y}N_{\psi''}-Y_{\psi''}N_{U'_Y}).\end{aligned}\right\} \tag{6.39}$$

The characteristic roots have one zero and either two real roots or one pair of complex roots. It is, thus, obvious that the yawing angle is indefinite without specifying initial condition. For stability in conventional configuration of the immersed vehicle, which has positive values of $(Y_{U'_Y}N_{\psi''}-Y_{\psi''}N_{U'_Y})$ and $2\zeta\omega_n$, the following condition must be satisfied:

$$Y_{U_Y}N_{\psi'}-Y_{\psi'}N_{U_Y}>0. \tag{6.40}$$

In an uncoordinated turning flight this must be

$$N_{\psi'}/N_{U_Y} > Y_{\psi'}/Y_{U_Y} = \partial \bar{U}_Y/\partial \psi' = (R/V_B^{1/3})(\Delta U_Y/U_{X,0}) \tag{6.41}$$

which is also approximated by

$$\bar{U}_{X,0}(C_{M_{Z,\psi'}}/C_{M_{Z,\beta}}) > (R/V_B^{1/3})(\Delta U_Y/U_{X,0}). \tag{6.42}$$

Usually the slender body configuration has nonlinear characteristics in yawing moment with respect to the side slip at small angle of side slip so that the derivative N_{U_Y} or C_{N_β} has a great variety of its value corresponding to the configuration and the side slip angle. Specifically for small tail fin configuration in small side slip the derivative sometimes takes a positive value so that the two roots might have a positive real part and, therefore, the vehicle is inherently unstable in lateral motion. This characteristic is, as the occasion may demand, required to get the quick response in the maneuver because a too stable vehicle will not turn as tight as a somewhat less stable vehicle. Then the vehicle must either install an automatic stability equipment in pilotless vehicle or be controlled in constant use of rudder by human pilot. If it is not so the vehicle will have a snaking motion eternally in such unstable region of side slip angle.

As stated before, since the differential drive of thrust produces not only turning moment but also change of longitudinal force the complete equations of motion in horizontal plane must be described by introducing the surging motion of the vehicle. This kind of motion will be treated in the subsequent section.

§7 Automatic Homing Control System

In order to know the position of the vehicle with respect to a coordinate fixer the vehicle provides three hydrophones and a signal processor. The hydrophones are arranged at the underside of the vehicle as shown in Fig. 2 and Table 9 and can receive a series of the ultrasonic signals which are generated every second at an acoustic generator of the coordinate fixer and propagated through the water. The signal processor can detect the time differences of signal reception among the three hydrophones and compute the vectorial position or distance and direction of the vehicle with respect to the signal generator or the coordinate fixer by knowing the depth and the attitude of the vehicle itself through the depth meter and a vertical gyro respectively.

Table 9 Relative of the hydrophones

Dimensional values		Nondimensional values	
$x_I - x_{III}$	2.03 m	$\bar{x}_I - \bar{x}_{III}$	1.338
y_I	0.4 m	$\bar{y}_I$	0.264
$z_I = z_Z$	0	$\bar{z}_I = \bar{z}_{II}$	0
z_{III}	0.05 m	$\bar{z}_{III}$	0.0330

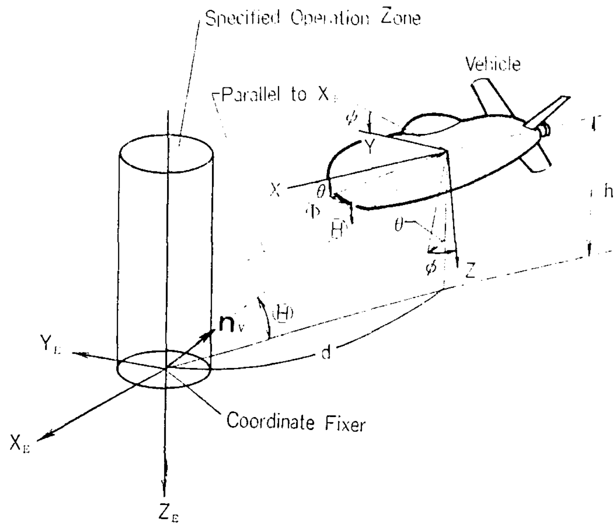

FIG. 10. Vehicle position in surveying area

In the present program of operation the vehicle has been required to stay in an imaginary cylinderical space the axis of which is standing uprightly on the coordinate fixer and the radius of which is specified by 25 m. (See Fig. 10)

By assuming the distance between the coordinate fixer and the vehicle, $\sqrt{d^2+h^2}$ is large enough comparing with the vehicle dimension, $V_B^{1/3}$, the acoustic wave from the generator may be considered a plane wave so that the time difference of signal reception between any couple of hydrophones is equivalent to the difference of relative distance along the direction of wave propagation between the said hydrophones. The relative positions of the hydrophones based on the No. 1 hydrophone can be expressed in the Earth coordinate system as follows:

$$\left.\begin{aligned} &\boldsymbol{r}_{\mathrm{I}}=0 \\ &\boldsymbol{r}_{\mathrm{II}}=\boldsymbol{T}_E(\Psi=\Psi_B)\cdot\boldsymbol{T}_B(\psi=0)\cdot(0,\ -2y_{\mathrm{I}},\ 0)^T \\ &\boldsymbol{r}_{\mathrm{III}}=\boldsymbol{T}_E(\Psi=\Psi_B)\cdot\boldsymbol{T}_B(\psi=0)\cdot(x_{\mathrm{III}}-x_{\mathrm{I}},\ -y_{\mathrm{I}},\ z_{\mathrm{III}}-z_{\mathrm{I}})^T. \end{aligned}\right\} \tag{7.1}$$

where Ψ_B is an angle of line-of-sight to the target measured from the longitudinal axis of the vehicle.

Since a unit vector from the coordinate fixer to the vehicle, $\boldsymbol{n}_V$, can be given by

$$\boldsymbol{n}_V=(-\cos\theta,0,\ -\sin\theta)^T \tag{7.2}$$

the time differences of the second and third hydrophones with respect to the first hydrophone can be given by

$$\left.\begin{aligned} t_{\mathrm{II}}&=\boldsymbol{r}_{\mathrm{II}}\cdot\boldsymbol{n}_V/c\cong 2y_{\mathrm{I}}\{(\cos\Psi_B\sin\phi\sin\theta-\sin\Psi_B\cos\phi)\cos\Theta+\sin\phi\cos\theta\sin\Theta\}/c \\ t_{\mathrm{III}}&=\boldsymbol{r}_{\mathrm{III}}\cdot\boldsymbol{n}_V/c\cong\{-(x_{\mathrm{III}}-x_{\mathrm{I}})\cos\Psi_B\cos\theta\cos\Theta \\ &\quad+y_{\mathrm{I}}(\cos\Psi_B\sin\phi\sin\theta-\sin\Psi_B\cos\phi)\cos\Theta \\ &\quad+(x_{\mathrm{III}}-x_{\mathrm{I}})\sin\theta\sin\Theta+y_{\mathrm{I}}\sin\phi\cos\theta\sin\Theta\}/c. \end{aligned}\right\} \tag{7.3}$$

By assuming that $\phi,\ \theta \ll 1$ the above equations yield

$$\left.\begin{aligned} ct_{\mathrm{II}}/2y_{\mathrm{I}} &\cong -\sin \Psi_B \cos \Theta + \phi \sin \Theta \\ ct_{\mathrm{III}}/(x_{\mathrm{III}}-x_{\mathrm{I}}) &\cong -\cos \Psi_B \cos \Theta - \{y_{\mathrm{I}}/(x_{\mathrm{III}}-x_{\mathrm{I}})\} \sin \Psi_B \cos \Theta + \theta \sin \Theta \\ &\quad + \{y_{\mathrm{I}}/(x_{\mathrm{III}}-x_{\mathrm{I}})\}\, \phi \sin \Theta. \end{aligned}\right\} \quad (7.4)$$

These relations give the following relations:

$$\left.\begin{aligned} \sin \Theta &= (ct_{\mathrm{II}}/2y_{\mathrm{I}})\phi + c(t_{\mathrm{III}}-t_{\mathrm{II}}/2)/(X_{\mathrm{III}}-x_{\mathrm{II}}) \\ &\quad \pm \sqrt{1-(ct_{\mathrm{II}}/2y_{\mathrm{I}})^2-\{c(t_{\mathrm{III}}-t_{\mathrm{II}}/2)/(x_{\mathrm{III}}-x_{\mathrm{II}})\}^2} \\ \cos \Theta &= \pm[\{(ct_{\mathrm{III}}/2y_{\mathrm{I}})-\phi \sin \Theta\}^2 + \{c(t_{\mathrm{III}}-t_{\mathrm{II}}/2)/(x_{\mathrm{III}}-x_{\mathrm{II}})-\theta \sin \Theta\}^2]^{1/2} \\ \sin \Psi_B &= \{\phi \sin \Theta - ct_{\mathrm{II}}/2y_{\mathrm{I}})\}/\cos \Theta \\ \cos \Psi_B &= \{\theta \sin \Theta - c(t_{\mathrm{III}}-t_{\mathrm{II}}/2)/(x_{\mathrm{III}}-x_{\mathrm{I}})\}/\cos \Theta \end{aligned}\right\} \quad (7.5)$$

and

$$d = h \cot \Theta. \quad (7.6)$$

The vertical motion and the trimming of the vehicle can be done by pumping in and out the water into a ballast tank and by shifting the mercury through front and rear tanks respectively. These operations are periodically performed by following to any one of presettled operation phases which can be selected by command signals sent from the data processing center on the land or ship via either buoy or mother ship by which the radio signals are transfered to the acoustic signals.

TABLE 10 Control algorithm in the automatic homing control system

<table>
<tr><td colspan="2" rowspan="2"></td><td rowspan="2">$\Psi_B > \Psi_{B1}$</td><td colspan="2">$\Psi_{B1} > \Psi_B \geq \Psi_{B2}$</td><td rowspan="2">$\Psi_{B2} > \Psi_B > -\Psi_{B2}$</td><td colspan="2">$-\Psi_{B2} > \Psi_B > -\Psi_{B1}$</td><td rowspan="2">$-\Psi_{B1} > \Psi_B$</td></tr>
<tr><td>$\dot{\Psi}_B < 0$</td><td>$\dot{\Psi}_B > 0$</td><td>$\dot{\Psi}_B < 0$</td><td>$\dot{\Psi}_B > 0$</td></tr>
<tr><td colspan="2">$d \geq d_1$</td><td colspan="3">Left turn</td><td colspan="2">Forward drive</td><td colspan="2">Right turn</td></tr>
<tr><td rowspan="2">$d_1 \geq d \geq d_2$</td><td>$\dot{d} < 0$</td><td colspan="3">$X_\delta = X_{\delta 2}$</td><td colspan="2">$X_\delta = X_{\delta 1}$</td><td colspan="2">$X_\delta = X_{\delta 2}$</td></tr>
<tr><td>$\dot{d} > 0$</td><td colspan="3">$N_\delta = -N_{\delta 0}$</td><td colspan="2">$N_\delta = 0$</td><td colspan="2">$N_\delta = +N_{\delta 0}$</td></tr>
<tr><td colspan="2">$d_2 > d$</td><td colspan="3">No control
$X_\delta = N_\delta = 0$</td><td colspan="2">No control
$X_\delta = N_\delta = 0$</td><td colspan="2">No control
$N_\delta = N_\delta = 0$</td></tr>
</table>

$\Psi_{B1} = 30°$, $\Psi_{B2} = 20°$, $d_1 = 15$ m, $d_2 = 10$ m

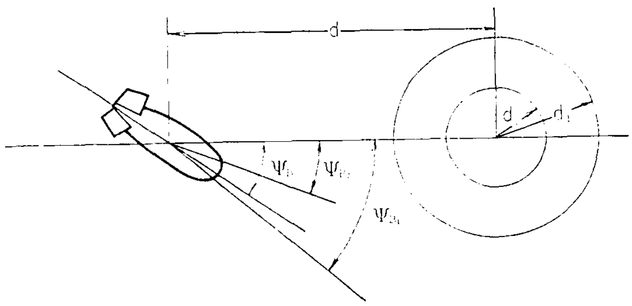

The control algorithm in the automatic homing control system is as follows: If the vehicle is in a target zone specified by a cylindrical space the both thrusters of the vehicle are stopped and the vehicle is therefore in state of no control. If the vehicle is, on the other hand, out of the target zone any of either right or left thruster is reversed and the vehicle makes right or left turn corresponding to the relative direction of the coordinate fixer with respect to the X-axis of the vehicle. By this operation if the relative direction of the vehicle is within a prescribed range the both thrusters are fully driven and the vehicle will approach to the target zone. Actually, there are, however, provided positively time lag for driving the thruster and hysteresis for making differential insentive zones in order to prevent the damage of electric motor of thruster and the batteries and to avoid unfavorable hunting respectively. That is to say, the thruster has the rest of two seconds at every switching of its rotational direction, and the insensitive zones of distance and direction have different levels for switching on and off as shown in Table 10.

The vehicle motion of the present problem can be represented by equations (6.9a), (6.10a) and (6.10c) as follows:

$$\left.\begin{aligned}
&(X_{U'_X}\bar{D}+X_{U_X})\Delta\bar{U}_X+X_{U_Y}\Delta U_Y+(X_{\psi''}\bar{D}^2+X_{\psi}D)\Delta\psi=X_\delta\\
&Y_{U_X}\Delta\bar{U}_X+(Y_{U'_Y}\bar{D}+Y_{U_Y})\Delta\bar{U}_Y+(Y_{\psi''}\bar{D}^2+Y_{\psi'}\bar{D}+Y_{\psi})\Delta\psi=0\\
&(N_{U'_X}\bar{D}+N_{U_X})\Delta\bar{U}_X+(N_{U'_Y}\bar{D}+N_{U_Y})\Delta\bar{U}_Y+(N_{\psi''}\bar{D}^2+N_{\psi'}\bar{D}+N_{\psi})\Delta\psi=N_\delta.
\end{aligned}\right\} \tag{7.7}$$

In these equations, the second term in the left hand side of the first equation and the first terms in the left hand side of the second and the third equations may be neglected as small quantities comparing with others. Thus the equations can be split further into the equation of pure surging and the coupled equations of swaying and yawing motions. Now, let us consider a case that the exemplified vehicle is in operation in a current, $W_{X,0}=-W$ and $W_{Y_0}=W_{Z_0}=0$, with zero speed with respect to the stationary axes or $U_{X,0}=U_{Y_0}=U_{Z_0}=0$ and with horizontal attitude, $\theta_0=0$.

A solution of the perturbed or maneuvered motion by a step input of turning command is as follows:

$$\left.\begin{aligned}
\Delta\bar{U}_X&=(X_\delta/X_{U_X})+\{\Delta U_{X_i}-(X_\delta/X_{U_X})\}e^{S_0 t}\\
\Delta U_Y&=A_0\Delta U_{Y,i}+B_0\Delta\psi_i+C_0\Delta\psi'_i+(D_0+E_0\bar{t})N_\delta\\
&\quad+(A_1\Delta U_{Y,i}+B_1\Delta\psi_i+C_1\Delta\psi'_i+D_1N_\delta)e^{S_1 t}\\
&\quad+(A_2\Delta U_{Y,i}+B_2\Delta\psi_i+C_2\Delta\psi'_i+D_2N_\delta)e^{S_2 t}\\
\Delta\psi&=k_1\{A_0\Delta U_{Y,i}+B_0\Delta\psi_i+C_0\Delta\psi_i+(k_0D_0+E_0\bar{t})N_\delta\}\\
&\quad+k_2(A_1\Delta U_{Y,i}+B_2\Delta\psi_i+C_1\Delta\psi'_i+D_1N_\delta)e^{S_1 t}\\
&\quad+k_3(A_2\Delta U_{Y,i}+B_2\Delta\psi_i+C_2\Delta\psi'_i+D_2N_\delta)e^{S_2 t}
\end{aligned}\right\} \tag{7.8}$$

where subscript i in $(\ )_i$ shows initial condition of $(\ )$, and where

$$
\left.
\begin{aligned}
&S_0 = -X_{U_X}/X_{U'_X} = -0.112\overline{W} \\
&\left.\begin{matrix} S_1 \\ S_2 \end{matrix}\right\} = (1/2)[(Y_{\psi''}N_{U_Y} + Y_{\psi'}N_{U'_Y} - Y_{U'_Y}N_{\psi''} - Y_{U'_Y}N_{\psi'}) \\
&\qquad \pm\{(Y_{\psi''}N_{U_Y} + Y_{\psi'}N_{U'_Y} - Y_{U_Y}N_{\psi''} - Y_{U'_Y}N_{\psi'})^2 - 4(Y_{U'_Y}N_{\psi''} - N_{U'_Y}Y_{\psi''}). \\
&\qquad (Y_{U_Y}N_{\psi'} + Y_{U'_Y}N_{\psi} - N_{U'_Y}Y_{\psi} - N_{U_Y}Y_{\psi'})\}^{1/2}]/(Y_{U'_Y}N_{\psi''} - N_{U'_Y}Y_{\psi''}) \\
&\quad = -1.024\overline{W} \text{ and } -0.370\overline{W}
\end{aligned}
\right\} \tag{7.9}
$$

$$
\left.
\begin{aligned}
&X_\delta/X_{U_X} = 0.480 \\
&A_0 = -0.999, \quad B_0 = 1.999, \quad C_0 = 1.202, \quad D_0 = -1.421/\overline{W}, \quad E_0 = 0.983 \\
&A_1 = -0.434, \quad B_1 = 0.434\overline{W}, \quad C_1 = -0.650, \quad D_1 = 0.589/\overline{W} \\
&A_2 = 2.433, \quad B_2 = -2.433\overline{W}, \quad C_2 = -0.549, \quad D_2 = 0.831/\overline{W} \\
&k_0 = 0.916/\overline{W}, \quad k_1 = 1/\overline{W}, \quad k_2 = 1.300/\overline{W}, \quad k_3 = 0.644/\overline{W}.
\end{aligned}
\right\} \tag{7.10}
$$

By applying the control algorithm to the above solution it will be expected to have limit cycles in the terminal area of the motion around the target zone. One possible cycle will be a symmetric lateral motion shown in Fig. 11.

The location of the vehicle in the horizontal plane and the angle of line-of-sight to the target can be given respectively by

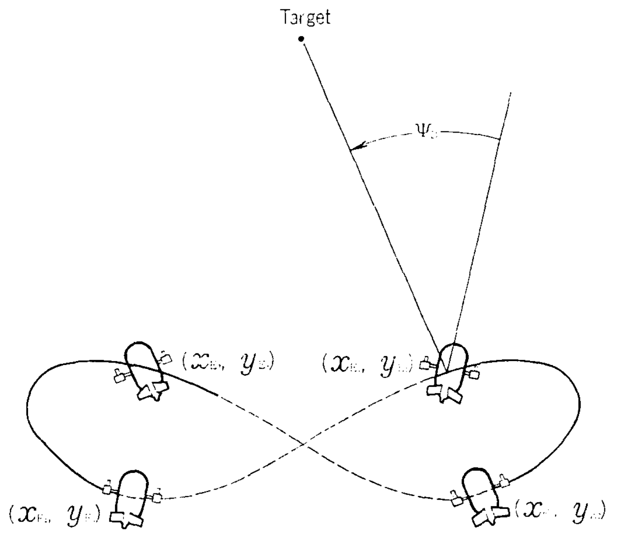

FIG. 11. A symmetric model of limit cycle

$$
\left.
\begin{aligned}
x_E &= \left\{\int (\Delta\bar{U}_X - \Delta\psi\Delta\bar{U}_Y)d\bar{t} + \bar{x}_{E_0}\right\} V_B^{1/3} \cong \left\{\int \Delta\bar{U}_X d\bar{t} + \bar{x}_{E_0}\right\} V_B^{1/3} \\
y_E &= \left\{\int (\Delta\psi\Delta\bar{U}_X + \Delta\bar{U}_Y)d\bar{t} + \bar{y}_{E_0}\right\} V_B^{1/3} \cong \left\{\int \Delta\bar{U}_Y d\bar{t} + \bar{y}_{E_0}\right\} V_B^{1/3}
\end{aligned}
\right\} \tag{7.11}
$$

$$
\Psi_B = \psi = \tan^{-1}(y_E/-x_E) \cong (\Delta U_Y/W) + \tan^{-1}(y_E/-x_E) \tag{7.12}
$$

where ΔU_X, ΔU_Y and $\Delta\psi$ have been assumed small. Referring to Fig. 11 the limit cycle will be specified as follows:

(i) Negative moment will be introduced at $(-x_{E1}, y_{E1})$
(ii) The moment will be released at $(-x_{E2}, y_{E2})$
(iii) Positive moment will be introduced at $(-x_{E3}, y_{E3})$
(iv) The moment will be released at $(-x_{E4}, y_{E4})$.

By imposing both symmetric conditions and the switching conditions on the solution given by equations (7.8) and (7.11–12) the limit cycle will be determined [8]. If the X coordinate of the switching points X_{E_1} and X_{E_2} are assumed to be $X_{E_1}=d_2$ and $X_{E_2}=d_1$ approximately, then the maximum lateral deviation in the limit cycls, $y_{E,\max}$, which can be obtained by solving $dx_E/dy=0$ at $y_E=y_{E,\max}$, by Fig. 12, in which a solid line shows the result obtained for two-seconds-rest of thrusters at switching point and a dotted line gives the result obtained for no rest of thrusters.

It is interesting to find that the maximum lateral deviation has a minimum value at a specific current speed and increases steeply as the current velocity decreases beyond the specified speed and that the two-seconds-rest of thrusters increases the deviation appreciable.

By investigating further the analytic solution for the above simplified model the following facts have been found: For higher current speed the effects of design control parameters such as hysteresises $\Psi_{B1}-\Psi_{B2}$ and d_1-d_2 are smaller than those for lower speed, and in the present system larger $\Psi_{B1}-\Psi_{B2}$ $(=15°)$ and smaller d_1-d_2 $(=2m)$ are necessary for better performance in lateral deviation.

In Fig. 12 there are also shown the results obtained from the simulation test of the unabridged equations of motion by means of the digital computer. They are split into two groups, the lower branch of which is close to the analytic solution and is obtained from the symmetric motion as shown in Fig. 13a and the upper branch of which is obtained from the larger side of asymmetric motion as shown in Fig. 13b. It is, thus, apparent that the simple analytic treatment is effective to examine the design parameters of the automatic homing control system.

Fig. 14 shows a typical example of the lateral orbit obtained by analyzing the tracking data of the exemplified vehicle during its actual operation in a test area

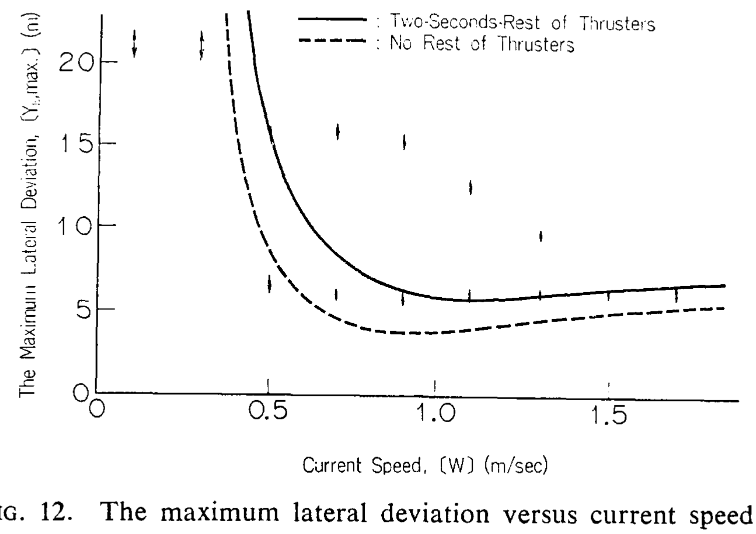

FIG. 12. The maximum lateral deviation versus current speed

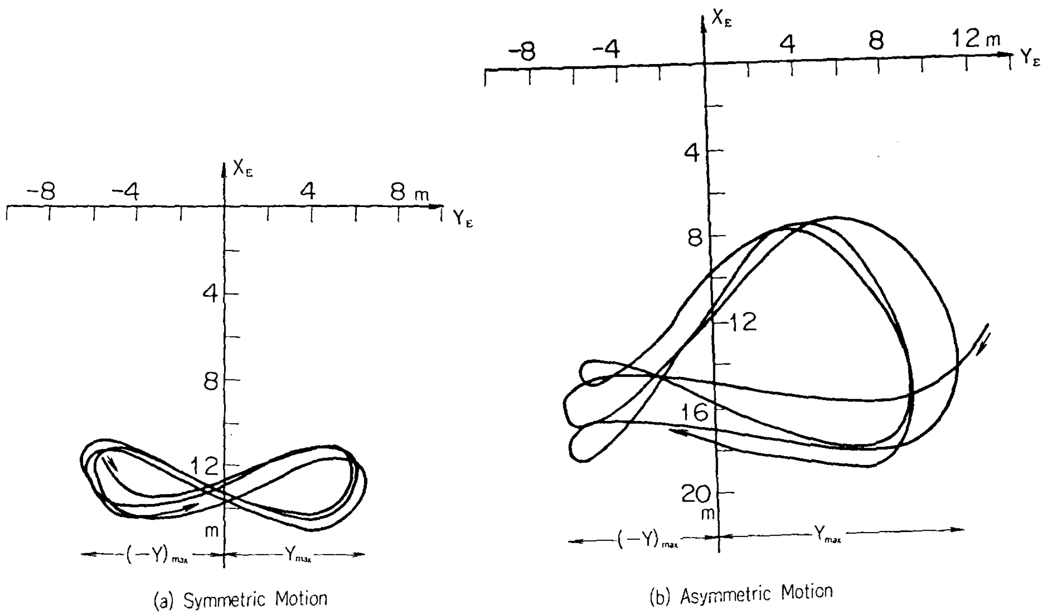

FIG. 13. Limit cycles in lateral motion obtained from the simulation test by means of the digital computer

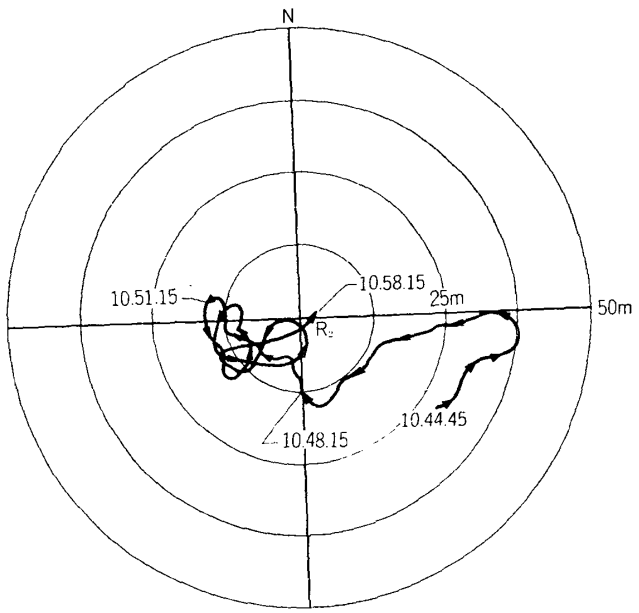

FIG. 14. Lateral motion in the operation test on October 25, 1975

at the Uchiura Bay. It is observed that the orbit of the vehicle in lateral plane shows similar behaviour to the computed result.

CONCLUSION

A short description has been presented on an ocean surveying vehicle which has been developed by the Japan Society for the Promotion of Machine Industry for obtaining oceanographic informations as a remotely piloted vehicle and was operated successfully at Uchiura Bay, Numazu City on November and December 1974.

The equations of motion of a general submersible have been given in the strict sense of the form. They were nondimensionalized by dividing with the buoyant force, $\rho g V_B$, for force balance and with its moment, $\rho g V_B^{4/3}$, for moment balance so that the equations of motion were treated universally in any flight speed including even hovering condition. By solving the stationary equations the performance of the exemplified vehicle was obtained. The flight dynamics of the vehicle has been discussed by getting linearized solutions of the perturbed motion of the vehicle. Some of design paramters of the automatic homing control system were also investigated by treating the simplified mathematical model of motion.

The comparison of the analytical results of the vehicle motion with those of simulation by means of digital computer was seen in very good coincidence. The experimental results on the vehicle motion obtained from the operational test in the sea showed similar behaviour to the computational results in the lateral motion.

Department of
Institute of Space and Aeronautical Science
University of Tokyo
February, 1977

REFERENCES

[1] Anon.: OSR System, Vol. 1, Development of Ocean Space Robot for Measurement of Oceanographic Parameters. Japan Society for the Promotion of Machine Industry. November, 1974.

[2] Anon.: OSR System, Vol. 2, Operation Tests and Evaluation of the System. Japan Society for the Promotion of Machine Industry.

[3] Streeter, Victor L. et al.: Handbook of Fluid Dynamics. McGraw-Hill Book Company, Inc. New York, 1961.

[4] Lass, Harry: Vector and Tensor Analysis. McGraw-Hill Book Company, Inc. New York, 1950.

[5] Küchemann, Dietrich and Weber, Johanna: Aerodynamics of Propulsion. McGraw-Hill Book Company, Inc., New York, 1953.

[6] Lamb, Horace: Helicopter Dynamics and Aerodynamics. Sir Isaac Pitman & Sons, Ltd., London, 1959.

[7] Lamb, Horace: Hydrodynamics. Combridge University Press, Fifth Edition, Cambridge, 1930.

[8] Nasu, Ken-ichi: Homing of Submersible by Means of Nonlinear Automatic Control System. Master Thesis, Aeronautical Course, Division of Engineering, University of Tokyo, March 1976.